haematologica
Journal of the Ferrata Storti Foundation

Gene expression profile of adult T-cell leukemia/lymphoma with human T-cell lymphotropic virus type 1-infected Hodgkin and Reed-Sternberg-like cells is more similar to classic Hodgkin lymphoma than typical adult T-cell leukemia/lymphoma

by Shohei Miyagi, Kyohei Mori, Kohta Miyawaki, Masatoshi Shimo, Tomoko Tamaki, Shugo Sakihama, Mitsuyoshi Takatori, Koichi Akashi, Kennosuke Karube and Koji Kato

Received: September 25, 2025.
Accepted: April 7, 2026.

Citation: Shohei Miyagi, Kyohei Mori, Kohta Miyawaki, Masatoshi Shimo, Tomoko Tamaki, Shugo Sakihama, Mitsuyoshi Takatori, Koichi Akashi, Kennosuke Karube and Koji Kato. Gene expression profile of adult T-cell leukemia/lymphoma with human T-cell lymphotropic virus type 1-infected Hodgkin and Reed-Sternberg-like cells is more similar to classic Hodgkin lymphoma than typical adult T-cell leukemia/lymphoma. Haematologica. 2026 Apr 16. doi: 10.3324/haematol.2025.289270 [Epub ahead of print]

Gene expression profile of adult T-cell leukemia/lymphoma with human T-cell lymphotropic virus type 1-infected Hodgkin and Reed-Sternberg-like cells is more similar to classic Hodgkin lymphoma than typical adult T-cell leukemia/lymphoma

Shohei Miyagi[1#], Kyohei Mori[2#], Kohta Miyawaki[2], Masatoshi Shimo[2], Tomoko Tamaki[3], Shugo Sakihama[4], Mitsuyoshi Takatori[5], Koichi Akashi[2], Kennosuke Karube[1$], Koji Kato[2$]

1. Department of Pathology and Laboratory Medicine, Graduate School of Medicine, Nagoya University, Nagoya, Japan.
2. Department of Medicine and Biosystemic Science, Kyushu University Graduate School of Medical Sciences, Fukuoka, Japan.
3. Department of Diagnostic Pathology, University of the Ryukyus Hospital, Okinawa, Japan.
4. Laboratory of Hematoimmunology, Graduate School of Health Sciences, University of the Ryukyus, Ginowan, Japan.
5. Department of Molecular and Cellular Physiology, Graduate School of Medicine, University of the Ryukyus, Ginowan, Japan.

#: These authors equally contributed to this study.

$: Corresponding authors

Correspondence

K. Karube and K. Kato

K. Karube - karube.kennosuke.x1@f.mail.nagoya-u.ac.jp

K. Kato kato.koji.429@m.kyushu-u.ac.jp

Disclosures

K. Karube has received honoraria from Janssen, Chugai, Takeda, Kyowa Kirin, Otsuka, AbbVie, Genmab, Eisai, AstraZeneca, SymBio, and Meiji-Seika Pharma, and research grant from Takeda and Eisai. The other authors have no conflicts of interest to disclose.

Funding

This study was supported by Grants-in-Aid for Scientific Research (KAKENHI) from the Ministry of Education, Culture, Sports, Science, and Technology of Japan (25K18745 [S.M.]

and 23K27384 [K. Karube]).

Contributions

S.M., K. Karube, K. Kato designed and conducted the research, reviewed all the cases, and wrote the manuscript. K. Mori, K. Miyawaki, and M.S. provided us with the genetically analyzed data. The other authors provided us with specimens, clinical information, or pathological evaluation. All authors read and approved the final version of this manuscript.

Data-sharing statement

The data that support the findings of this study are available from the corresponding author upon reasonable request.

Adult T-cell leukemia/lymphoma (ATLL) is a mature T-cell neoplasm associated with human T-cell leukemia virus type 1 (HTLV-1) infection.[1] The most common histological pattern is diffuse proliferation of pleomorphic tumor cells, but several other histological variations are recognized.[1] Classic Hodgkin lymphoma (CHL) is a B-cell lymphoma with characteristic Hodgkin and Reed-Sternberg (HRS) cells. Using a new sensitive method that can detect HTLV-1 viral products on formalin-fixed paraffin-embedded (FFPE) samples, in situ hybridization for HTLV-1 basic zipper factor (HBZ-ISH)[2], we identified a new histological pattern termed ATLL with HTLV-1-infected HRS-like cells (ATLL-HH).[2] ATLL-HH is considered a unique histological pattern of ATLL, with neoplastic HTLV-1-positive HRS-like cells and non-neoplastic inflammatory cells, histologically mimicking CHL.[2] Similar to HRS cells in CHL, HRS-like cells in ATLL-HH express CD30 and CD15, but they are usually negative for PAX5 and often CD4-positive.[2] The tumor microenvironment (TME) differs in terms of both quantity and quality between ATLL and CHL.[3, 4] In this study, we explored the pathological characteristics of both tumor cells and the TME of ATLL-HH based on their comprehensive gene expression profiles to elucidate where ATLL-HH is pathologically located on the spectrum between typical ATLL and CHL.

We analyzed 12 samples from 11 patients (1 recurrent case) of ATLL-HH. The diagnosis of ATLL-HH was based on the detection of HBZ-ISH-positive signals in HRS-like cells using FFPE samples. The clinicopathological findings in six cases (no. 1, 3-7; Supplementary Table 1A) were reported in a previous study.[2] We also analyzed eight CHL cases and six typical ATLL cases. The CHL cases included three HTLV-1 carriers and five HTLV-1-negative patients (Supplementary Table 1B). Among three cases of CHL arising from HTLV-1 carriers, we confirmed that HRS cells were HTLV-1-negative by HBZ-ISH, and the two cases for which clonality analysis was available had a polyclonal pattern for TRG rearrangement. Gene expression analysis using nCounter (NanoString Technologies, Seattle, WA) and the PanCancer Immune Profiling panel (770 genes) was performed for FFPE samples as described previously.[5] The clustering analysis and analysis of differentially expressed genes were carried out using nSolver Analysis Software (https://nanostring.com/). Gene enrichment analysis was performed using Enrichr.[6] For immunohistochemical evaluation of TBET and IDO1, all pairwise comparisons were carried out using the Mann-Whitney U test in EZR.[7] This study was approved by the Institutional Review Board of Nagoya University (2022-0406).

The clustering analysis (Fig. 1A) demonstrated that ATLL-HH had analogous gene expression profiles and was grouped within the same cluster as CHL, regardless of the EBV status of the CHL. In contrast, typical ATLL formed a distinct cluster. Supplementary Table 2 shows the top 30 genes upregulated in ATLL-HH and CHL compared to typical ATLL. GO biological process pathway enrichment analysis (Fig. 1B) demonstrated that 8 of the 10 pathways in ATLL-HH compared to typical ATLL were identical to those in CHL. The transcription factor protein-protein interaction (PPI) analysis identified involvement of the JAK/STAT pathway in both ATLL-HH and CHL (Fig. 1C). Based on these findings, we focused on CCL17, STAT6, TBET, and IDO1, all of which had significantly elevated expression in ATLL-HH and CHL compared to typical ATLL (Fig. 2A). The localization of these proteins was analyzed by immunohistochemistry in the seven ATLL-HH cases, five CHL cases, and five typical ATLL cases for which additional materials were available (Fig. 3A-D). We analyzed phosphorylated STAT6 (pSTAT6) instead of total STAT6 to more accurately assess the activation of the JAK-STAT6 pathway. HRS(-like) cells were positive for CCL17 in five of seven ATLL-HH cases and in all five CHL cases. Similarly, pSTAT6 expression was observed in HRS(-like) cells in all seven ATLL-HH cases and in all four evaluable CHL cases; one case was not evaluable. CCL17 expression was largely restricted to HRS(-like) cells, whereas pSTAT6 positivity was also observed in a subset of lymphocyte-like and endovascular cells, consistent with previous reports.[8] In contrast, none of the typical ATLL cases exhibited pSTAT6- or CCL17-positive tumor cells. The lower expression levels of CCL17 and STAT6 in typical ATLL than in ATLL-HH and CHL, as demonstrated by gene expression profiling, may reflect the absence of HRS(-like) cells in typical ATLL. TBET expression was observed mainly in lymphocytes, but also in HRS(-like) cells (30-80%) in all cases of ATLL-HH and CHL. Morphologically, IDO1-positive cells were considered to be macrophages/dendritic cells, and no IDO1-positive HRS(-like) cells were observed. The numbers of TBET-positive and IDO1-positive TME cells were significantly higher in ATLL-HH and CHL than in typical ATLL (Fig. 2B, 3A-D).

CCL17 is a chemokine that HRS cells in CHL produce and contributes to the T-cell-rich TME.[9] HRS cells reportedly express CCL17 in 85% of CHL cases.[10] In our study, HRS-like cells in ATLL-HH were positive for CCL17, which suggests that they had similar characteristics to HRS cells in CHL. STAT6 is a representative transcription factor in the JAK/STAT pathway.

In 87% of CHL cases, HRS cells have been shown to have genetic dysregulation in the JAK/STAT pathway.[11] Immunohistochemical pSTAT6 positivity in HRS cells was useful in distinguishing CHL from other histological mimickers.[12] Our immunohistochemical analysis revealed that HRS-like cells in ATLL-HH expressed pSTAT6, suggesting the importance of the JAK/STAT pathway in its pathogenesis similar to CHL, as shown in the PPI analysis based on the gene expression profile. TBET is a transcription factor important for the differentiation of CD4-positive T cells into Th1 T cells. The TME of CHL consists of various cells, including T cells, especially Th1 T cells, and CHL cases with more TBET-positive cells have been reported to have better disease-specific survival.[13] We found numerous TBET-positive cells in the TME of ATLL-HH, suggesting a Th1-dominant TME in ATLL-HH similar to CHL. IDO1 is an enzyme in the kynurenine pathway and a recently studied immunosuppressive molecule. Overexpression of IDO1 in macrophages and dendritic cells in the TME suppresses effector T-cell function and induces Tregs, resulting in immune tolerance.[14] Regarding the TME of CHL, cases with more IDO1-positive macrophages have a worse prognosis.[14] Significantly more IDO1-positive cells were found in the TME of ATLL-HH than in typical ATLL, suggesting that they play a role in the tumorigenesis of ATLL-HH through immune tolerance.

One limitation of our study is the lack of comprehensive clinical information; therefore, the prognostic significance of the gene expression profiles remains unclear. Nevertheless, as shown in Supplementary Table 1A, ATLL-HH was associated with relatively high serum LDH and sIL-2R levels, as well as frequent extranodal involvement. These findings may provide supportive information for distinguishing ATLL-HH from CHL, although their diagnostic utility requires validation in larger studies. Another unresolved issue is the cellular origin of HRS-like cells in ATLL-HH. Although five cases showed a clonal peak within a predominantly polyclonal background-including cases in which the HRS-like cells were positive for PAX5-these findings alone are insufficient to establish the lineage of HRS-like cells in the absence of single-cell-based analyses (Supplementary Table 1A and Supplementary Figure 1). A third limitation is that Hodgkin-like ATLL,[15] which has been reported to occur in HTLV-1 carriers with CHL-like morphology, was not included in this study. The morphology and number of atypical cells around HRS-like cells in Hodgkin-like ATLL were diverse (data not shown), and it was often difficult to clearly distinguish them from CHL or typical ATLL. Further accumulation of cases and integrated

analysis of Hodgkin-like ATLL are in progress.

In conclusion, comprehensive gene expression profiling revealed that ATLL-HH shares a molecular signature with CHL. This similarity appears to be attributed to CCL17 expression and STAT6 activation in HRS-like cells, along with the presence of numerous TBET-positive Th1 cells and IDO1-positive cells in the TME. These shared pathological features may support common therapeutic strategies targeting both ATLL-HH and CHL.

References

1. Karube K MH, Cook LB, et al. Adult T-cell leukemia/lymphoma. In: board WCoTE, ed. WHO classification of tumors, haematolymphoid tumours, 5th ed. Lyon, France: WHO Press. 2024:p. 667-673.

2. Karube K, Takatori M, Sakihama S, et al. Clinicopathological features of adult T-cell leukemia/lymphoma with HTLV-1-infected Hodgkin and Reed-Sternberg-like cells. Blood Adv. 2021;5(1):198-206.

3. Nakahata S, Enriquez-Vera D, Jahan MI, Sugata K, Satou Y. Understanding the Immunopathology of HTLV-1-Associated Adult T-Cell leukemia/lymphoma: a comprehensive review. Biomolecules. 2023;13(10):1543.

4. Duffield AS, Ascierto ML, Anders RA, et al. Th17 immune microenvironment in Epstein-Barr virus-negative Hodgkin lymphoma: implications for immunotherapy. Blood Adv. 2017;1(17):1324-1334.

5. Miyawaki K, Kato K, Sugio T, et al. A germinal center-associated microenvironmental signature reflects malignant phenotype and outcome of DLBCL. Blood Adv. 2022;6(7):2388-2402.

6. Chen EY, Tan CM, Kou Y, et al. Enrichr: interactive and collaborative HTML5 gene list enrichment analysis tool. BMC Bioinformatics. 2013;14:128.

7. Kanda Y. Investigation of the freely available easy-to-use software 'EZR' for medical statistics. Bone Marrow Transplant. 2013;48(3):452-458.

8. Skinnider BF, Elia AJ, Gascoyne RD, et al. Signal transducer and activator of transcription 6 is frequently activated in Hodgkin and Reed-Sternberg cells of Hodgkin lymphoma. Blood. 2002;99(2):618-626.

9. Kilsdonk M, Veldman C, Rosati S, Plattel W, Diepstra A. The value of thymus and activation related chemokine immunohistochemistry in classic Hodgkin lymphoma diagnostics. Histopathology. 2023;82(3):495-503.

10. Peh SC, Kim LH, Poppema S. TARC, a CC chemokine, is frequently expressed in classic Hodgkin's lymphoma but not in NLP Hodgkin's lymphoma, T-cell-rich B-cell lymphoma, and most cases of anaplastic large cell lymphoma. Am J Surg Pathol. 2001;25(7):925-929.

11. Tiacci E, Ladewig E, Schiavoni G, et al. Pervasive mutations of JAK-STAT pathway genes in classical Hodgkin lymphoma. Blood. 2018;131(22):2454-2465.

12. Satou A, Takahara T, Yamashita D, et al. Diagnostic utility of STAT6 and pSTAT6

Immunohistochemistry for distinguishing classic hodgkin lymphoma and peripheral T-Cell lymphoma with hodgkin and Reed-Sternberg-like cells. Am J Surg Pathol. 2023;47(8):897-906.

13. Greaves P, Clear A, Owen A, et al. Defining characteristics of classical Hodgkin lymphoma microenvironment T-helper cells. Blood. 2013;122(16):2856-2863.

14. Choe JY, Yun JY, Jeon YK, et al. Indoleamine 2,3-dioxygenase (IDO) is frequently expressed in stromal cells of Hodgkin lymphoma and is associated with adverse clinical features: a retrospective cohort study. BMC Cancer. 2014;14:335.

15. Ohshima K, Kikuchi M, Yoshida T, Masuda Y, Kimura N. Lymph nodes in incipient adult T-cell leukemia-lymphoma with Hodgkin's disease-like histologic features. Cancer. 1991;67(6):1622-1628.

Figure legends

Figure 1

Comprehensive RNA expression analysis by nCounter. (A) Cluster analysis of the gene expression profiles of ATLL with HTLV-1-infected HRS-like cells (ATLL-HH), classic Hodgkin lymphoma (CHL), and typical adult T-cell leukemia/lymphoma (ATLL). Arrows indicate EBV negative CHL. Arrowheads indicate the primary and relapsed lesions of the same case. (B) Gene enrichment analysis of ATLL-HH, CHL, and typical ATLL by Enrichr using GO Biological Process 2023. (C) Gene enrichment analysis of ATLL-HH, CHL, and typical ATLL by Enrichr using transcription factor protein-protein interactions (PPIs).

Figure 2

Expression analysis of CCL17, STAT6, TBET and IDO1. (A) Boxplot of CCL17, STAT6, TBET, and IDO1 RNA expression. (B) Number of TBET-positive and IDO1-positive cells by immunohistochemistry. The average number of positive cells in three high-power fields (x400) was calculated. TBET-positive HRS(-like) cells were excluded. *$p<0.05$.

Figure 3

Representative immunostaining images. (A) CCL17, (B) pSTAT6, (C) TBET, and (D) IDO1 in ATLL with HTLV-1-infected HRS-like cells (ATLL-HH), classic Hodgkin lymphoma (CHL), and typical adult T-cell leukemia/lymphoma (ATLL)

A

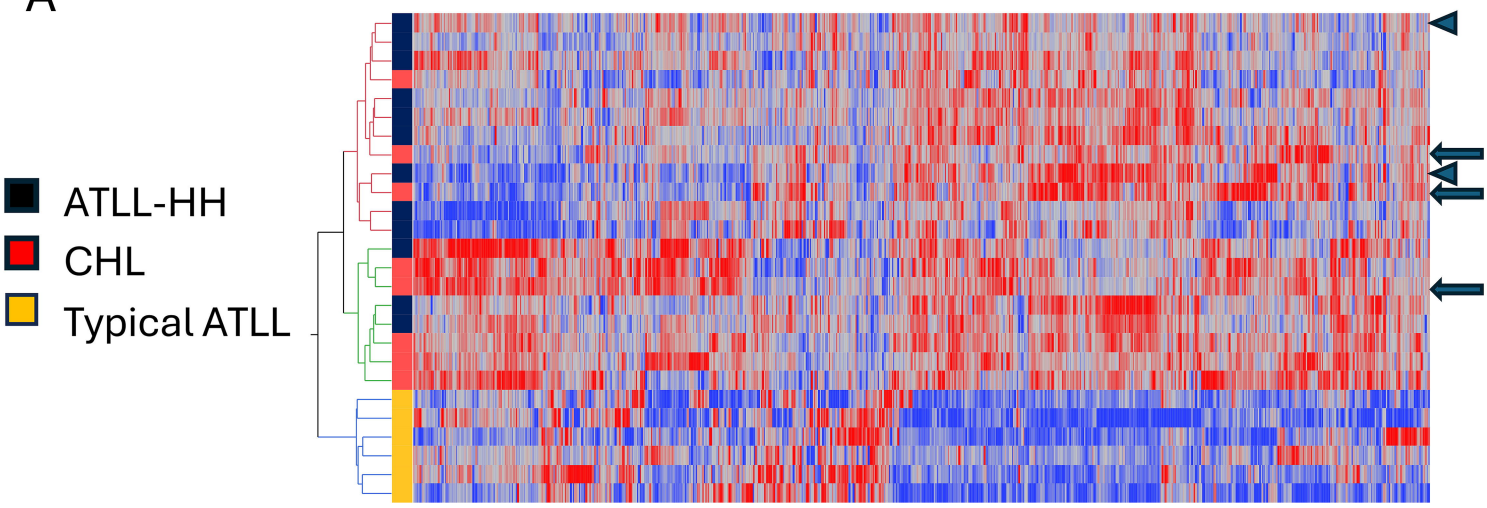
ATLL-HH
CHL
Typical ATLL

B

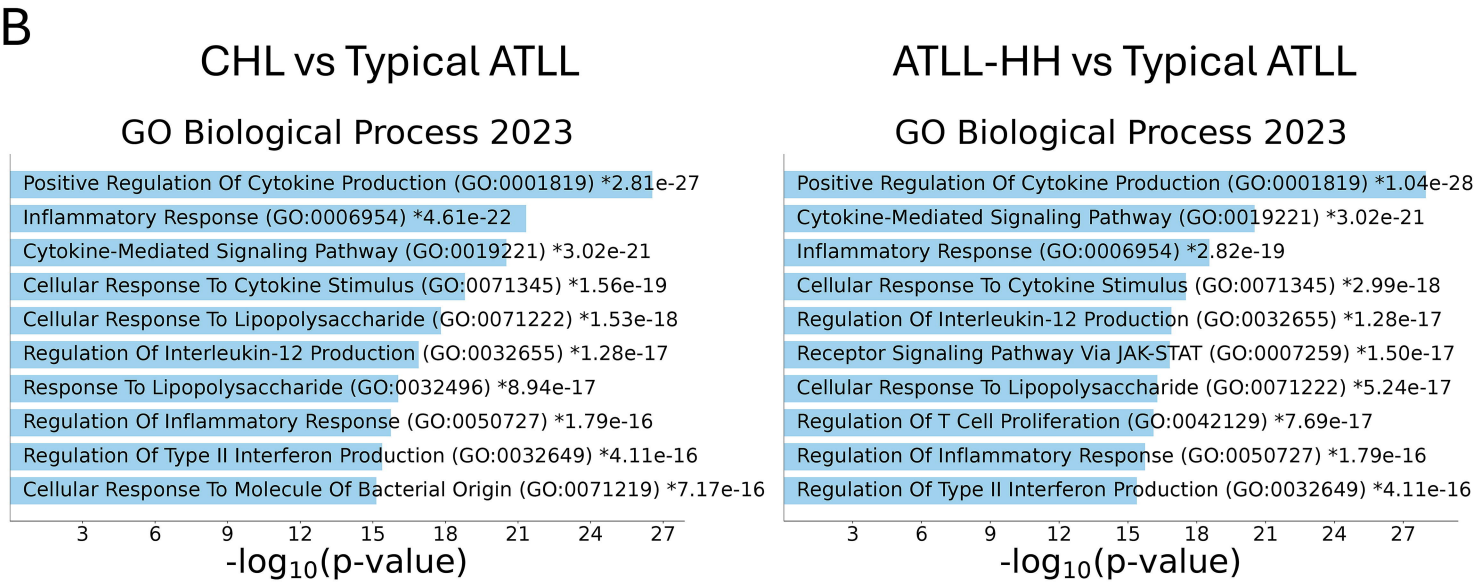
CHL vs Typical ATLL
GO Biological Process 2023
Positive Regulation Of Cytokine Production (GO:0001819) *2.81e-27
Inflammatory Response (GO:0006954) *4.61e-22
Cytokine-Mediated Signaling Pathway (GO:0019221) *3.02e-21
Cellular Response To Cytokine Stimulus (GO:0071345) *1.56e-19
Cellular Response To Lipopolysaccharide (GO:0071222) *1.53e-18
Regulation Of Interleukin-12 Production (GO:0032655) *1.28e-17
Response To Lipopolysaccharide (GO:0032496) *8.94e-17
Regulation Of Inflammatory Response (GO:0050727) *1.79e-16
Regulation Of Type II Interferon Production (GO:0032649) *4.11e-16
Cellular Response To Molecule Of Bacterial Origin (GO:0071219) *7.17e-16
3 6 9 12 15 18 21 24 27
-log10(p-value)
ATLL-HH vs Typical ATLL
GO Biological Process 2023
Positive Regulation Of Cytokine Production (GO:0001819) *1.04e-28
Cytokine-Mediated Signaling Pathway (GO:0019221) *3.02e-21
Inflammatory Response (GO:0006954) *2.82e-19
Cellular Response To Cytokine Stimulus (GO:0071345) *2.99e-18
Regulation Of Interleukin-12 Production (GO:0032655) *1.28e-17
Receptor Signaling Pathway Via JAK-STAT (GO:0007259) *1.50e-17
Cellular Response To Lipopolysaccharide (GO:0071222) *5.24e-17
Regulation Of T Cell Proliferation (GO:0042129) *7.69e-17
Regulation Of Inflammatory Response (GO:0050727) *1.79e-16
Regulation Of Type II Interferon Production (GO:0032649) *4.11e-16
3 6 9 12 15 18 21 24 27
-log10(p-value)

C

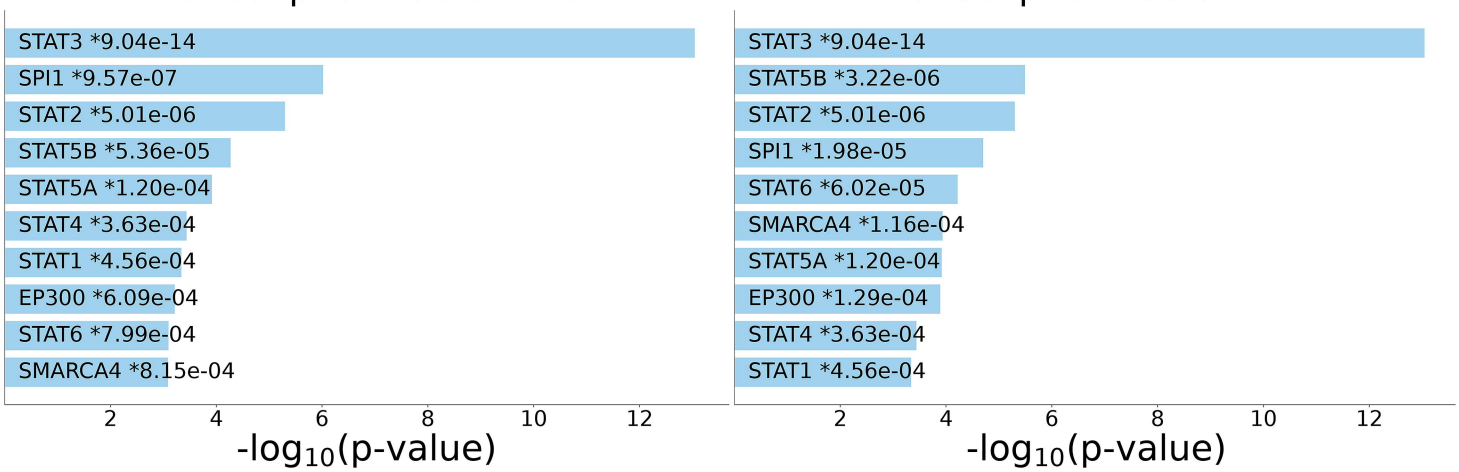
CHL vs Typical ATLL
Transcription Factor PPIs
STAT3 *9.04e-14
SPI1 *9.57e-07
STAT2 *5.01e-06
STAT5B *5.36e-05
STAT5A *1.20e-04
STAT4 *3.63e-04
STAT1 *4.56e-04
EP300 *6.09e-04
STAT6 *7.99e-04
SMARCA4 *8.15e-04
2 4 6 8 10 12
-log10(p-value)
ATLL-HH vs Typical ATLL
Transcription Factor PPIs
STAT3 *9.04e-14
STAT5B *3.22e-06
STAT2 *5.01e-06
SPI1 *1.98e-05
STAT6 *6.02e-05
SMARCA4 *1.16e-04
STAT5A *1.20e-04
EP300 *1.29e-04
STAT4 *3.63e-04
STAT1 *4.56e-04
2 4 6 8 10 12
-log10(p-value)

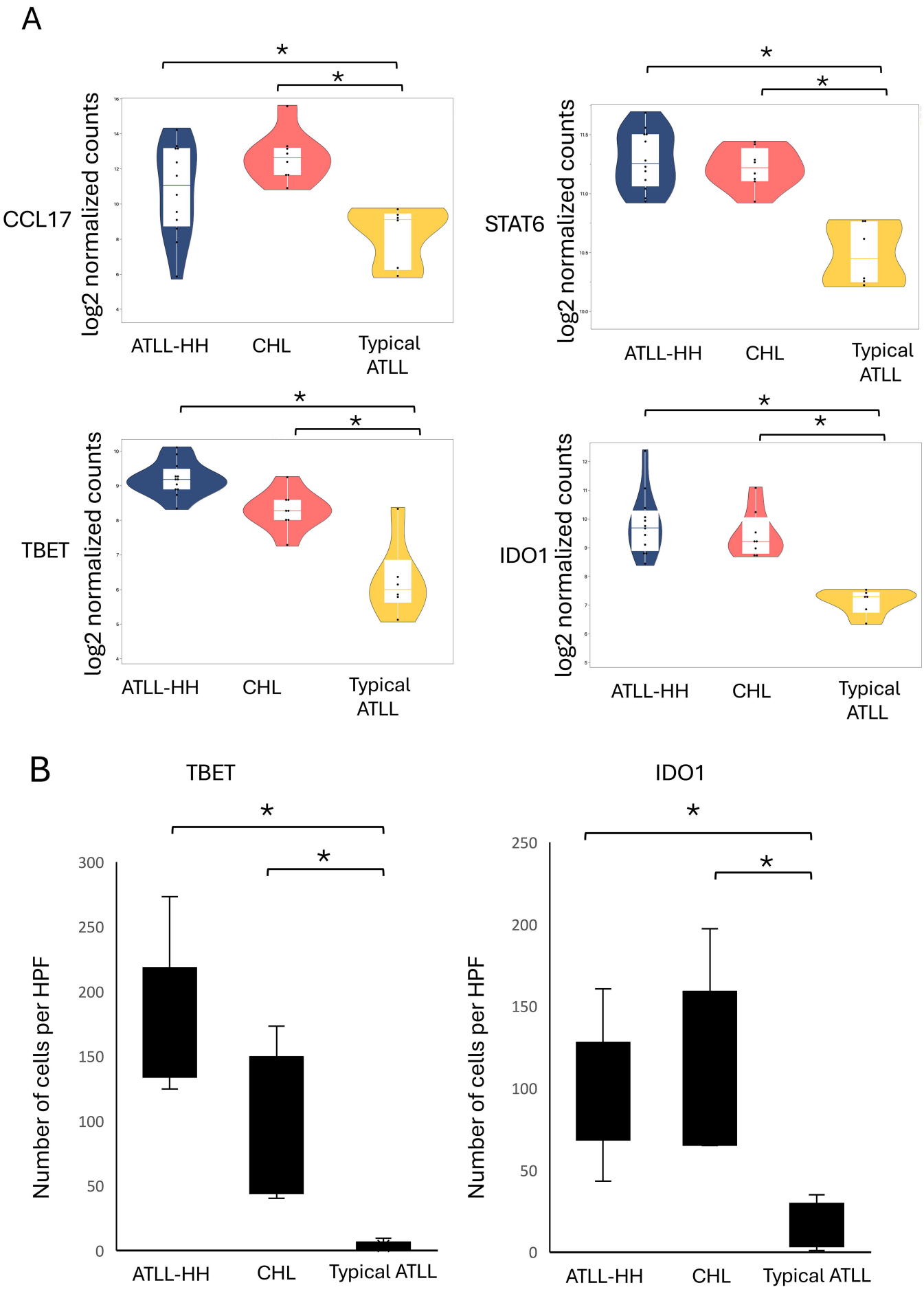
A
CCL17
log2 normalized counts
ATLL-HH
CHL
Typical ATLL
STAT6
log2 normalized counts
ATLL-HH
CHL
Typical ATLL
TBET
log2 normalized counts
ATLL-HH
CHL
Typical ATLL
IDO1
log2 normalized counts
ATLL-HH
CHL
Typical ATLL
B
TBET
Number of cells per HPF
ATLL-HH
CHL
Typical ATLL
IDO1
Number of cells per HPF
ATLL-HH
CHL
Typical ATLL

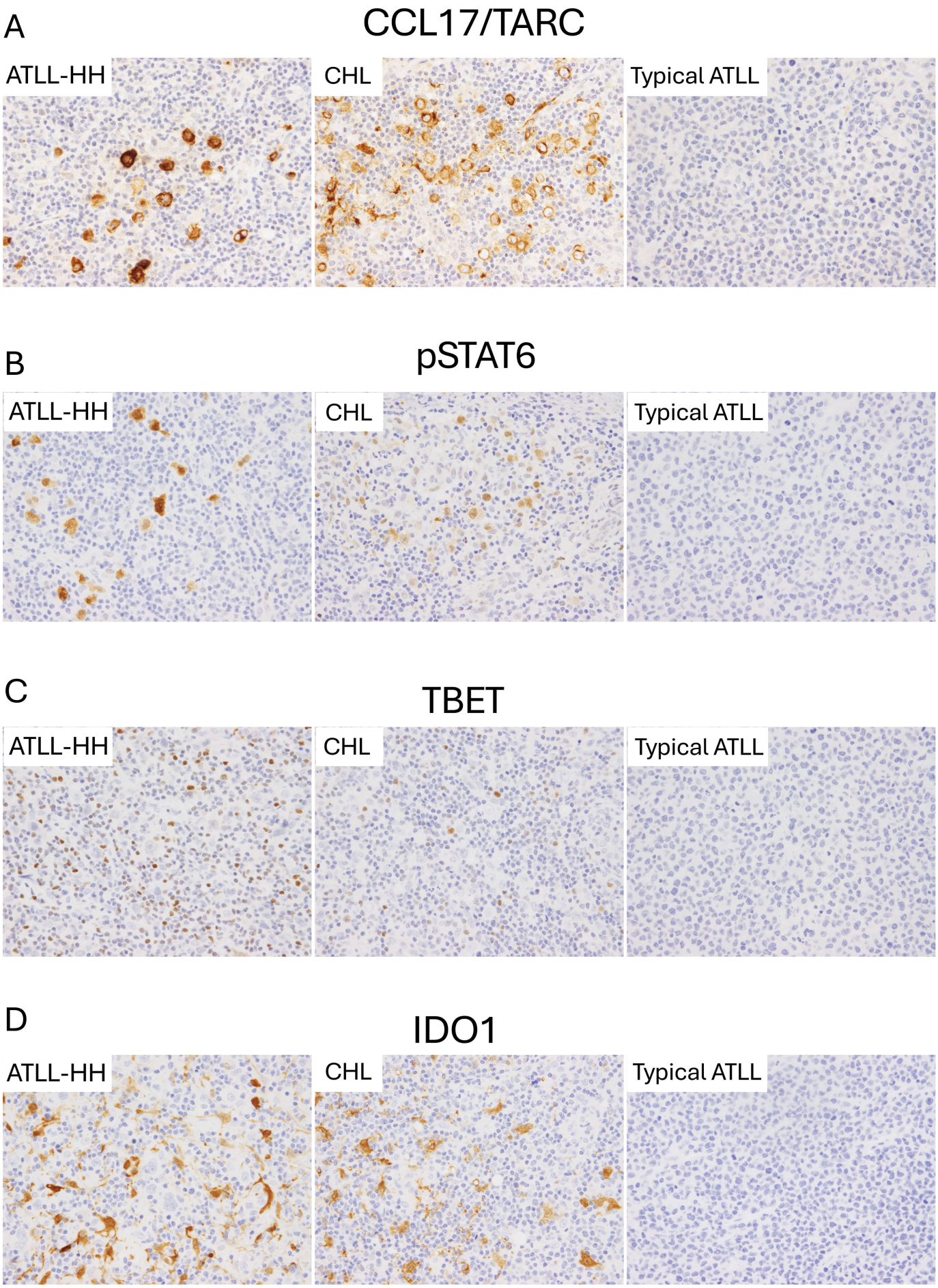
A
CCL17/TARC
ATLL-HH
CHL
Typical ATLL
B
pSTAT6
ATLL-HH
CHL
Typical ATLL
C
TBET
ATLL-HH
CHL
Typical ATLL
D
IDO1
ATLL-HH
CHL
Typical ATLL

Supplementary Table 1 Clinicopathological characteristics of ATLL-HH, CHL and typical ATLL

1A. Clinicopathological characteristics of ATLL-HH

Case no.	Clinical characteristics								Pathological characteristics of HRS-like cells														
	Age (years)/sex	Background status	Ann Arbor stage	LDH, U/L	sIL-2R, U/mL	Alb, g/dL	Ca, mg/dL	Extranodal involvement	Histology	CD30	CD15	PAX5	BOB1	OCT2	CD3	CD20	CD5	CD7	TIA-1	CD4	HBZ-ISH	EBER-ISH	TRG
1[a]	69/M	Smoldering type[b]	IV	332	6502	3.6	11.7	Skin, Spleen, BM	MC like	+	+	-	-	-	-	-	-	-	-	+, f	+	-	polyclonal
2	Recurrent case of no. 1 (two years later)	NA	NA	156	31911	1.6	8.9	NA	MC like	+	+	-	NA	NA	-	-	-	-	NA	+, f	+	-	NA
3	55/M	HTLV-1 carrier	I	255	4667	4.4	8.9	None	MC like	+	+	-	-	-	-	-	NA	-	-	+	+	-	polyclonal
4[a]	79/F	HTLV-1 carrier	IV	331	7618	2.2	7.9	Liver, Spleen, Bone	MC vs. NS	+	+, f	-	-	-	-	-	-	-	-	-	+	-	polyclonal
5[a]	80/F	HTLV-1 carrier	II	307	9240	3.6	8.6	None	MC like	+	+, f	-	-	-	-	-	-	-	-	-	+	-	NE
6[a]	72/F	HTLV-1 carrier	II	299	2493	2.9	8.7	None	MC like	+	+, f	-	-	-	-	-	-	-	-	+	+	-	clonal[c]
7[a]	81/M	HTLV-1 carrier	III	465	34772	2.5	7.5	Spleen	MC like	+	+, f	-	-	-	-	-	-	-	-	+, f	+	-	clonal[c]
8	70/F	HTLV-1 carrier	IV	306	4294	2.5	8.1	BM, Liver, Spleen	MC like	+	+	-	-		-	-	-	-	-	+	+	-	clonal[c]
9[a]	79/F	HTLV-1 carrier	IV	306	4294	3.7	9.0	Spleen, Bone	MC like	+	+	-	-	-	-	-	-	-	-	-	+	-	polyclonal
10[a]	75/M	HTLV-1 carrier	II	197	1166	3.7	9.7	None	MC like	+	+	+	-	+, f	-	-	-	-	-	+, f	+	-	clonal[c]
11	65/F	HTLV-1 carrier	IV	232	5403	3.7	8.8	Spleen, Bone	MC like	+	+, f	+	+	+, f	-	-	NA	NA	NA	+, f	+	-	polyclonal
12	82/M	HTLV-1 carrier	II	200	1375	3.6	8.8	None	MC like	+	+	+, f	-	-	-	-	NA	NA	-	-	+	-	clonal[c]

All ATLL-HH cases were serological HTLV-1(+).

[a]Validated by immunohistochemistry of CCL17, pSTAT6, TBET, and IDO1.

[b]10 years prior to the diagnosis of ATLL-HH.

[c]Monoclonal peak was identified with polyclonal backgrounds.

Alb, albumin; ATLL-HH, adult T-cell leukemia/lymphoma with HTLV-1-infected HRS-like cells; BM, Bone marrow; Ca, calcium; f, focal (10%-30% of cells positive); F, female; LDH, lactate dehydrogenase; M, male; MC, mixed cellularity; NA, not assessed; NE, not evaluable; NS, nodular sclerosis; sIL-2R, soluble interleukin 2 receptor; TRG, TCR-γ chain gene.

Supplementary Table 1 Clinicopathological characteristics of ATLL-HH, CHL and typical ATLL

1B. Clinicopathological characteristics of CHL and typical ATLL

Case no.	Clinical characteristics			Pathological characteristics			
	Diagnosis	Age (years)/sex	HTLV-1 antibody	Histology	HBZ-ISH	EBER-ISH	TRG
13	CHL	73/F	+	MC	-[b]	+[c]	polyclonal
14[a]	CHL	61/F	+	MC	-[b]	+[c]	NE
15[a]	CHL	36/M	-	MC	NA	+[c]	NA
16[a]	CHL	38/M	-	MC	NA	-[c]	NA
17	CHL	40/F	-	NS	NA	-[c]	NA
18[a]	CHL	28/M	-	NS	NA	-[c]	NA
19[a]	CHL	78/M	-	MC	NA	+[c]	NA
20	CHL	78/M	+	NS	-[b]	+[c]	polyclonal
21	Typical ATLL	56/M	+	large anaplastic	NA	NA	NA
22[a]	Typical ATLL	58/M	+	medium pleomorphic	NA	NA	NA
23[a]	Typical ATLL	52/F	+	large pleomorphic	NA	NA	NA
24[a]	Typical ATLL	75/F	+	medium pleomorphic	NA	NA	NA
25[a]	Typical ATLL	72/F	+	large pleomorphic	NA	NA	NA
26[a]	Typical ATLL	84/F	+	large pleomorphic	NA	NA	NA

[a]Validated by immunohistochemistry of CCL17, pSTAT6, TBET, and IDO1.

[b,c]In CHL cases, the evaluation of HBZ-ISH and EBER-ISH was performed on HRS cells.

ATLL, adult T-cell leukemia/lymphoma; CHL, classic Hodgkin lymphoma; F, female; M, male; MC, mixed cellularity; NA, not assessed; NE, not evaluable; NS, nodular sclerosis; TRG, TCR-γ chain gene.

Supplementary Table 2 Top 30 genes upregulated in ATLL-HH and CHL compared to typical ATLL

ATLL-HH			CHL		
Gene symbol	Log2 fold change	BY.p.value	Gene symbol	Log2 fold change	BY.p.value
CXCL9	4.76	1.82E-05	S100A8	6.28	6.21E-05
IL21	4.64	6.32E-07	KLRB1	4.78	3.11E-05
CXCL13	4.42	0.00013	CD7	3.69	2.67E-08
CHIT1	4.36	0.000461	CXCR6	3.53	1.59E-06
KLRB1	4.23	3.12E-05	SLAMF1	3.44	1.59E-06
HSD11B1	4.11	6.11E-06	CCR5	3.31	2.51E-06
HAMP	4.03	0.00129	CXCR3	3.1	2.44E-06
C4B	3.94	7.02E-06	SLAMF7	2.99	2.33E-05
CR2	3.8	0.0041	TLR2	2.79	1.52E-05
SLAMF7	3.79	2.16E-07	TNFSF13	2.54	4.14E-05
GZMH	3.76	1.83E-05	TNFSF8	2.54	6.23E-05
TLR8	3.72	1.61E-06	CSF2RB	2.53	3.20E-06
CD7	3.56	6.44E-09	MAF	2.5	5.95E-06
CXCR6	3.52	2.07E-07	CSF1R	2.41	1.52E-05
CCR5	3.51	2.14E-07	HCK	2.36	1.51E-05
SLAMF1	3.47	2.07E-07	LYN	2.36	1.82E-05
CCL17	3.47	0.00785	CD40	2.32	3.58E-06
S100A8	3.44	0.00982	CD84	2.3	2.48E-06
IFNG	3.4	8.04E-07	CYBB	2.3	1.33E-05
CCL18	3.28	0.0188	TLR4	2.25	1.33E-05
C1QB	3.25	3.31E-05	CCR2	2.1	3.11E-05
CXCR3	3.24	2.14E-07	CMKLR1	1.99	3.71E-05
IDO1	3.24	3.66E-05	ICAM1	1.94	1.67E-05
CXCL11	3.13	0.00159	STAT4	1.89	1.59E-06
LILRB1	3.12	1.89E-06	IRF8	1.86	4.41E-05
POU2AF1	3.07	0.000348	LTBR	1.86	6.21E-05
IL6	3.06	0.00472	TLR1	1.82	1.67E-05

TNFSF8	3.05	1.31E-06	IL10RA	1.76	2.06E-05
CXCL10	3.04	0.00433	PRKCD	1.32	4.75E-05
CCL23	3.03	0.0462	RELB	1.25	3.26E-05

ATLL-HH, adult T-cell leukemia/lymphoma with HTLV-1-infected HRS-like cells; CHL, classic Hodgkin lymphoma; ATLL, adult T-cell leukemia/lymphoma.

Supplementary Figure 1 TRG clonality assay of ATLL-HH.
The X-axis indicates the size of the amplicons, and the Y-axis indicates fluorescent signal intensity. The blue arrow shows the size range of the amplicons that can be evaluated.

case 1 TRG(A)

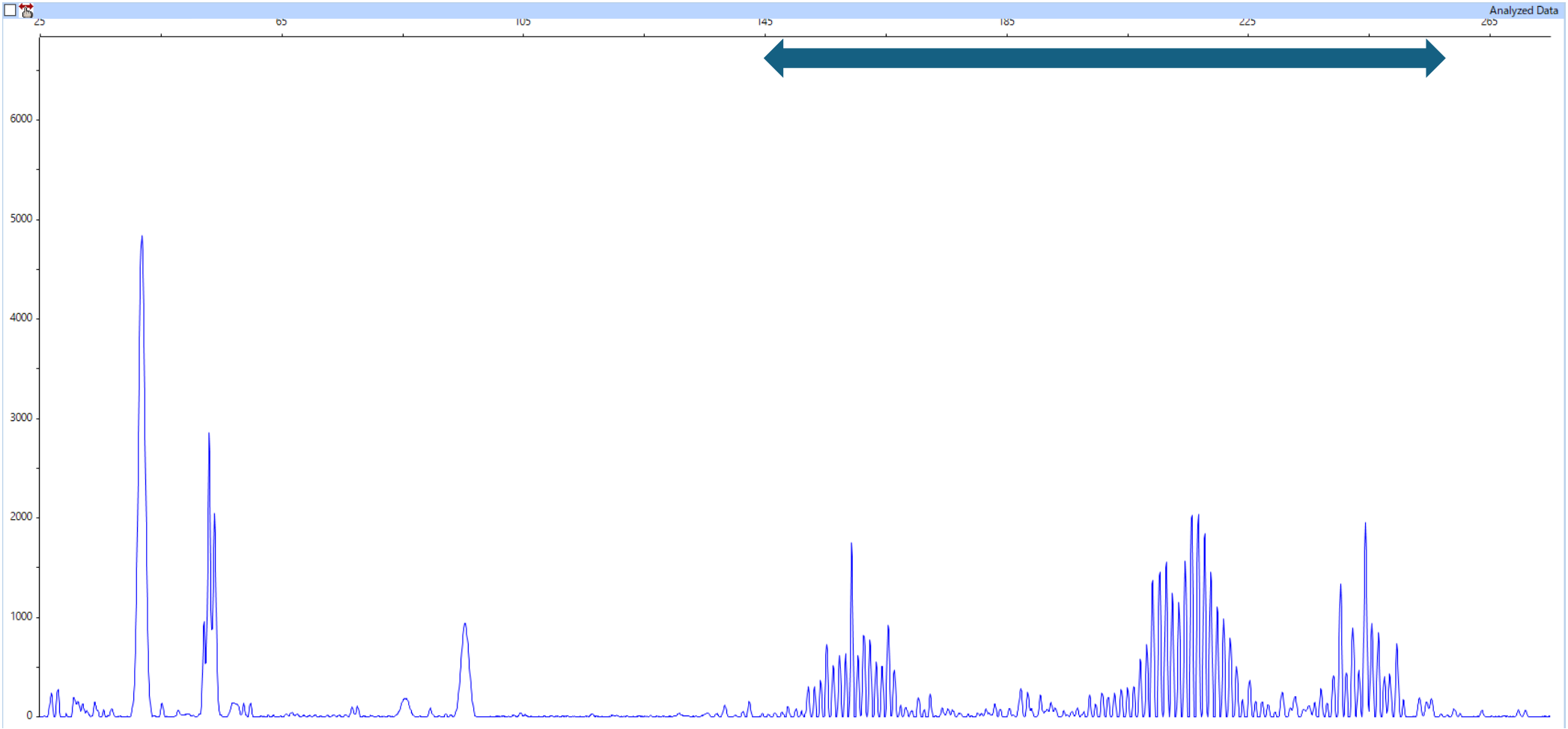
Analyzed Data
25
65
105
145
185
225
265
6000
5000
4000
3000
2000
1000
0

case 1 TRG(B)

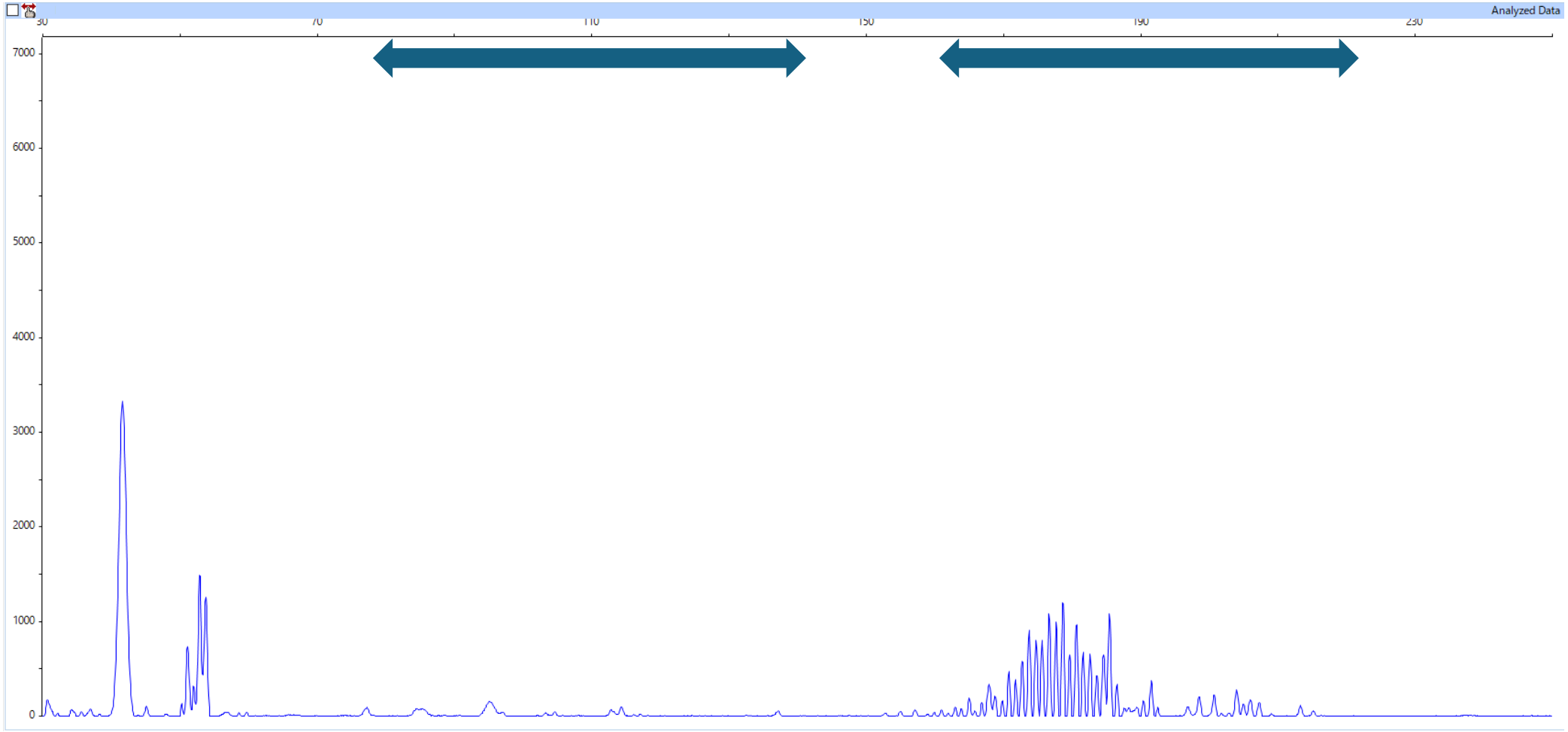
Analyzed Data
70
110
150
190
230
7000
6000
5000
4000
3000
2000
1000
0

case 3 TRG(A)

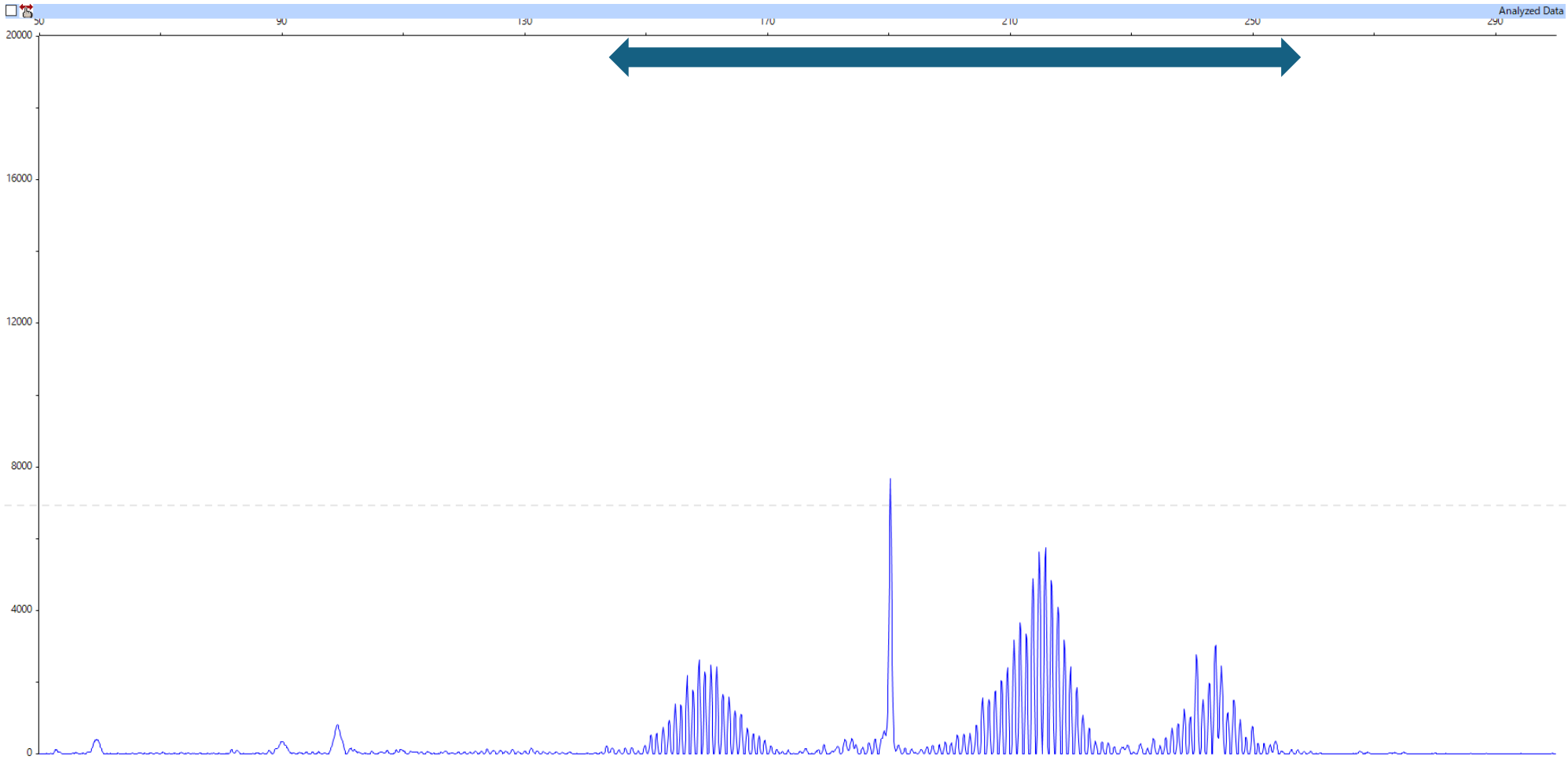
Analyzed Data
50
90
130
170
210
250
290
20000
16000
12000
8000
4000
0

case 3 TRG(B)

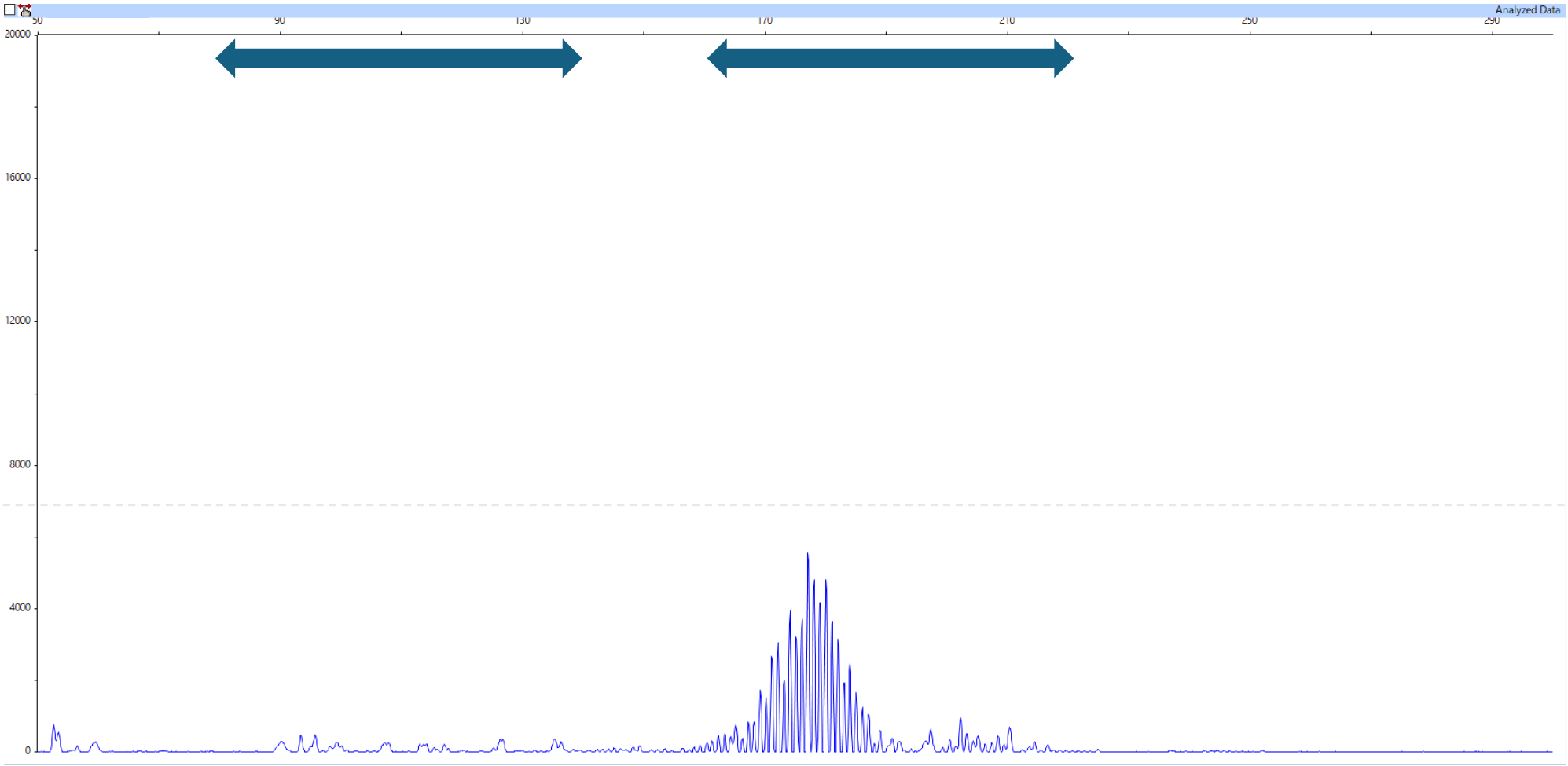
Analyzed Data
50
90
130
170
210
250
290
20000
16000
12000
8000
4000
0

case 4 TRG(A)

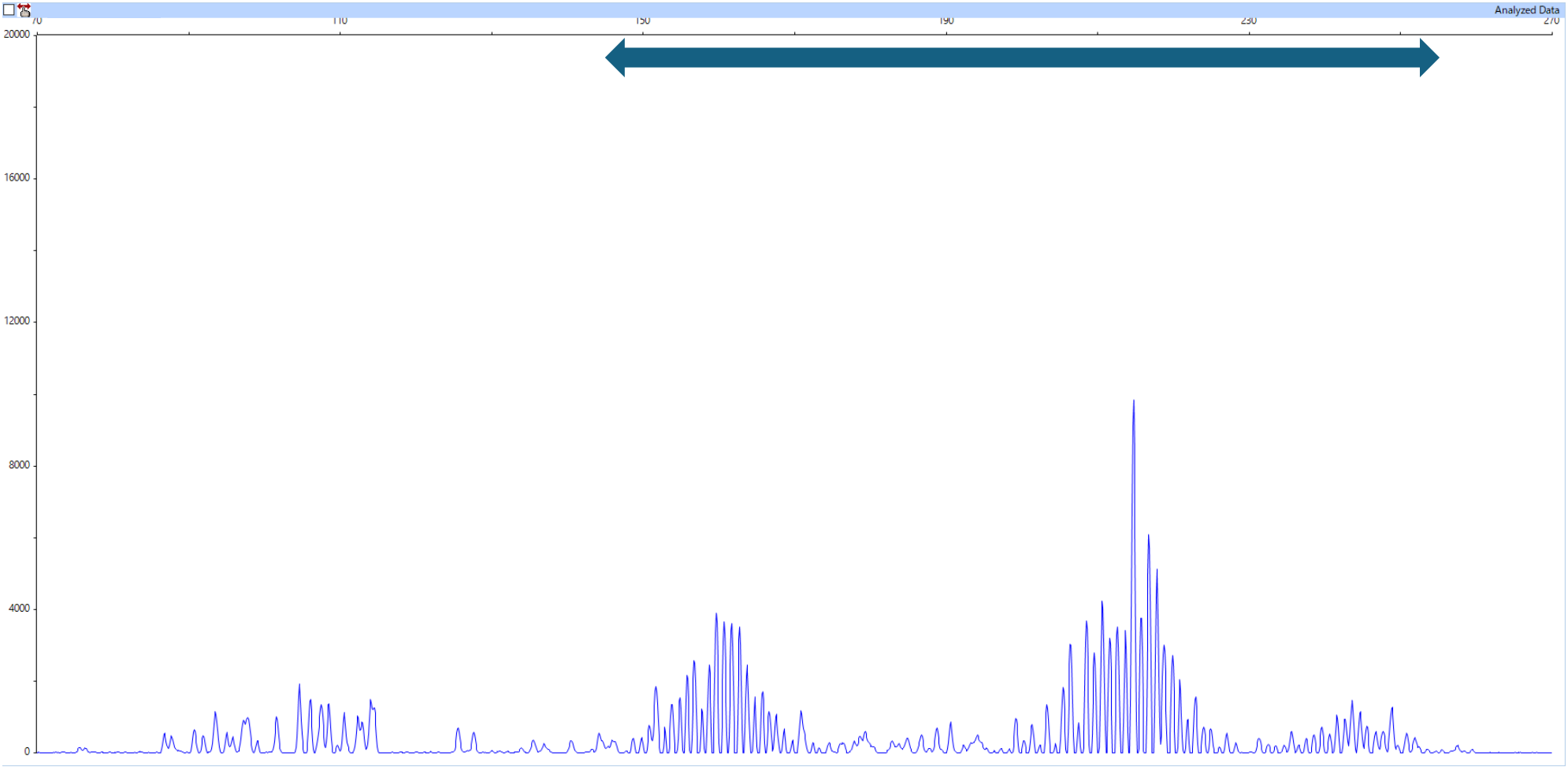
Analyzed Data
70
110
150
190
230
270
20000
16000
12000
8000
4000
0

case 4 TRG(B)

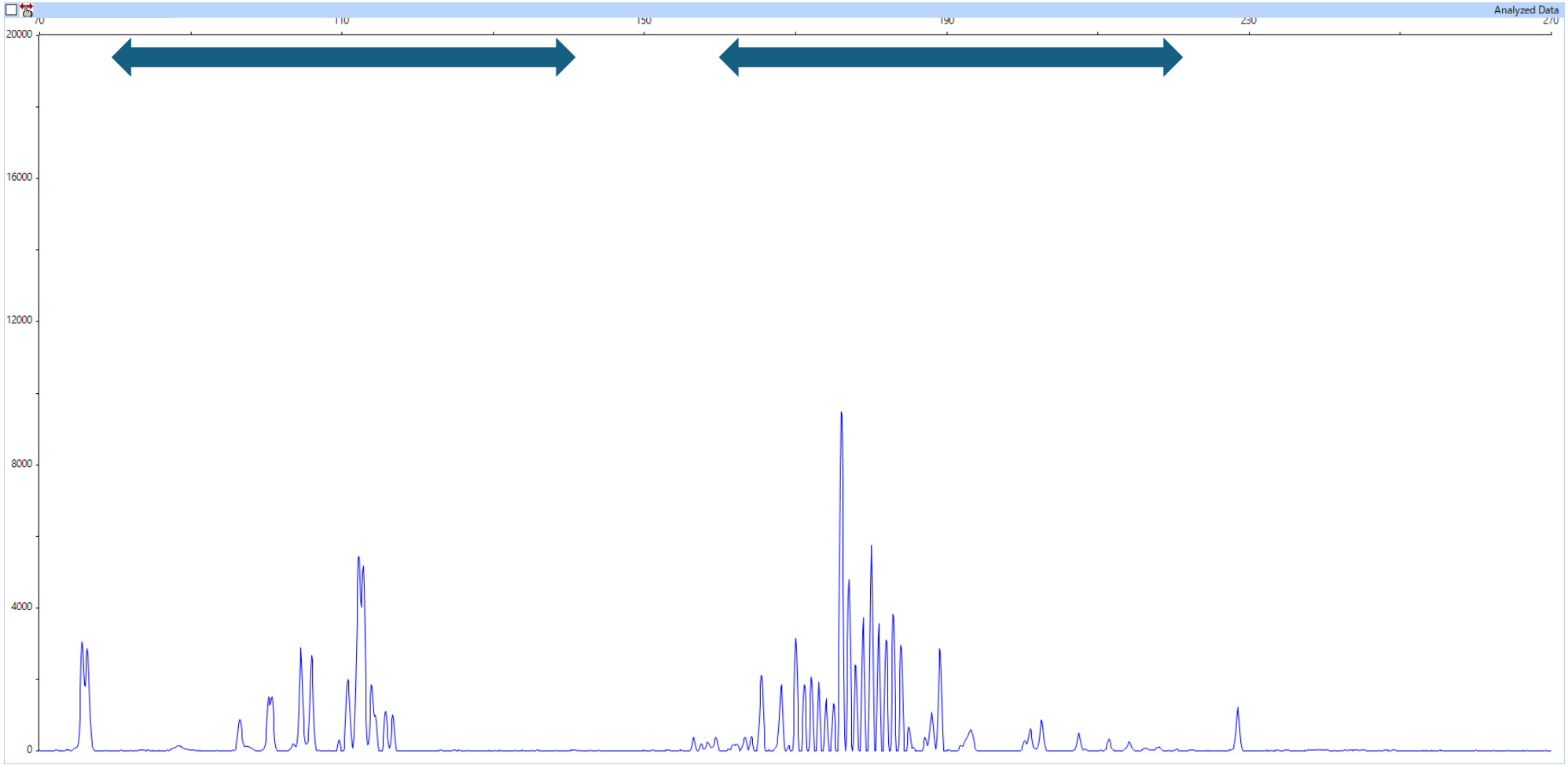
Analyzed Data
70
110
150
190
230
270
20000
16000
12000
8000
4000
0

case 6 TRG(A)

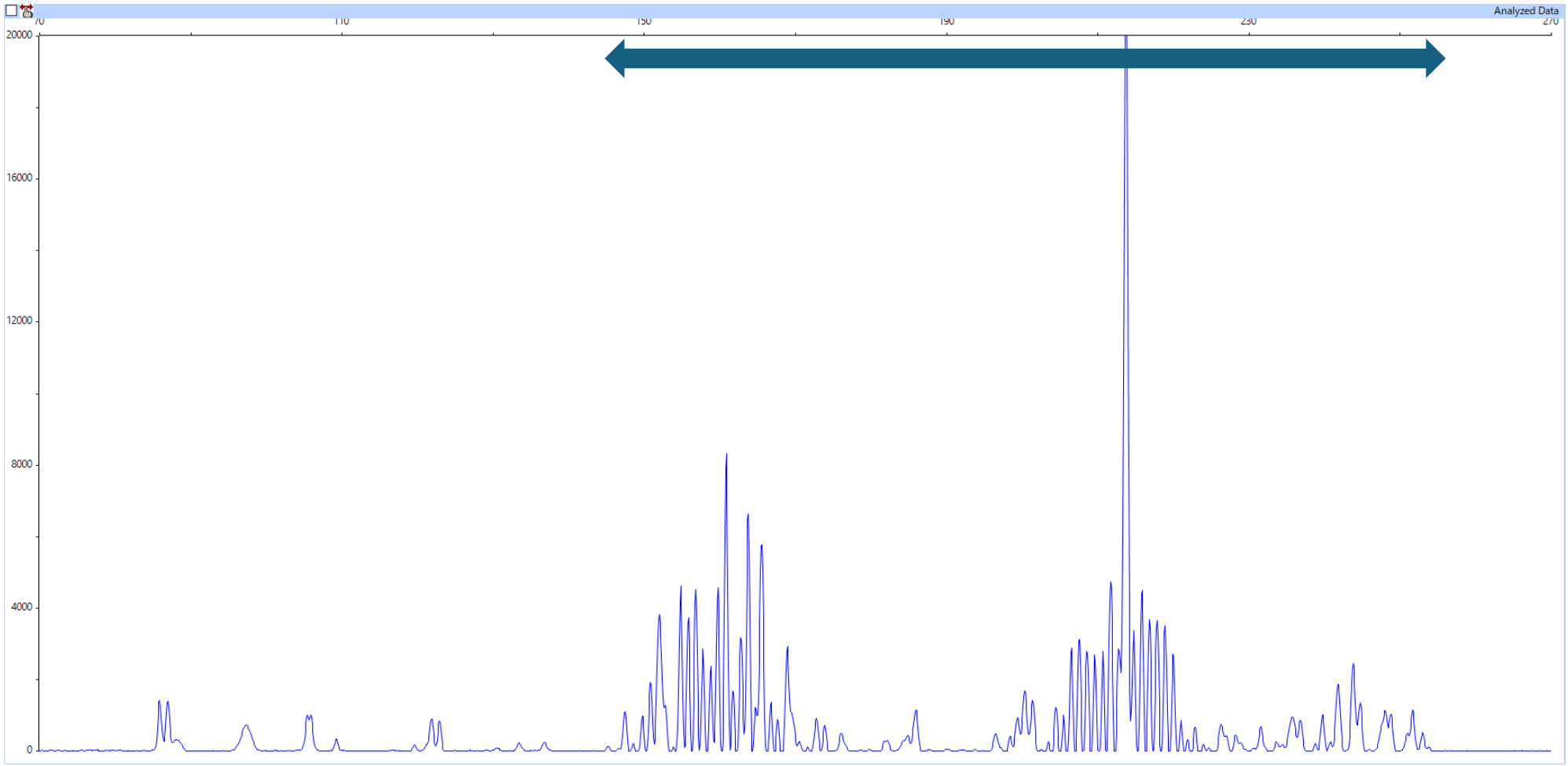
Analyzed Data
70
110
150
190
230
270
20000
16000
12000
8000
4000
0

case 6 TRG(B)

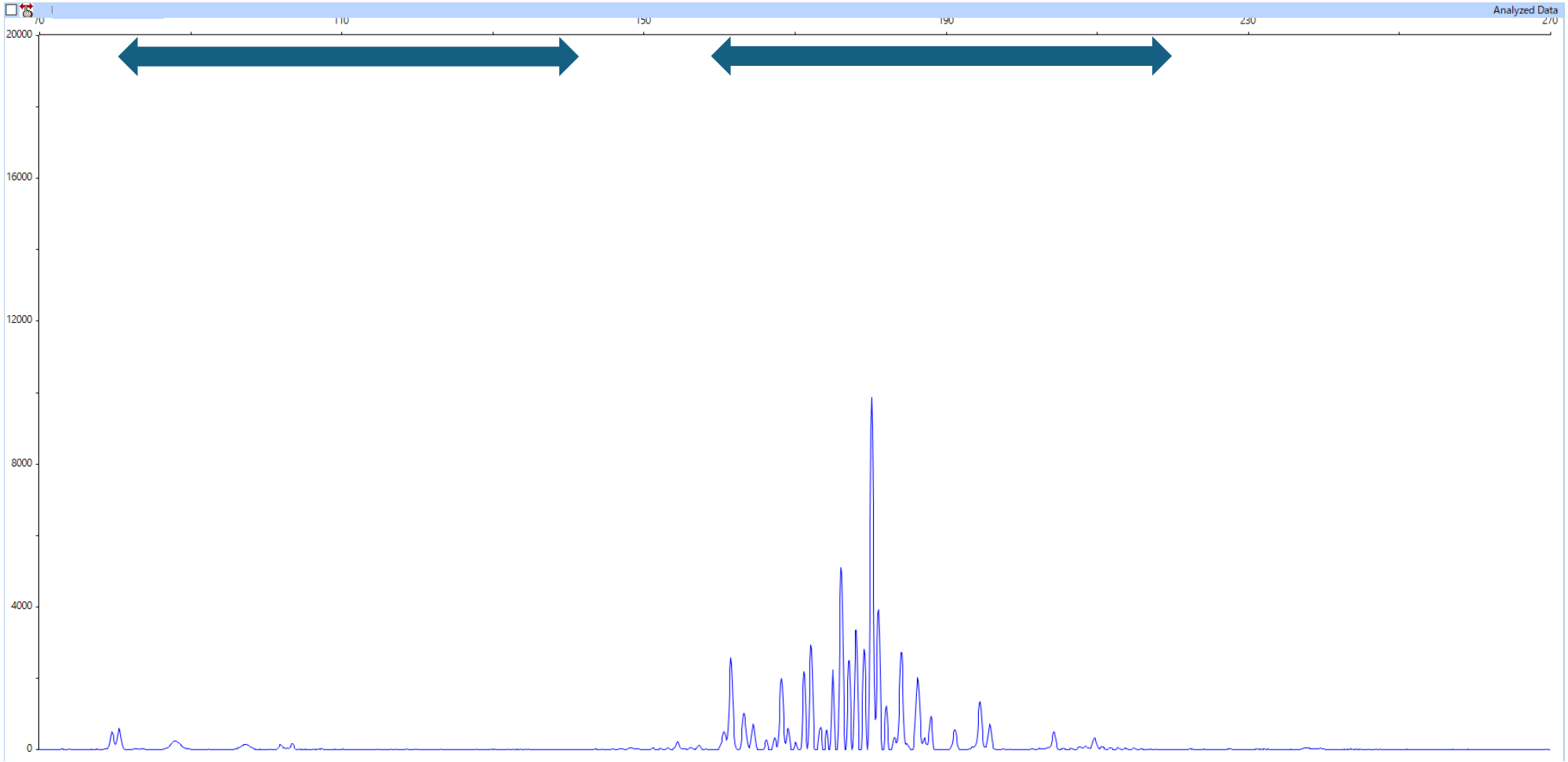
Analyzed Data
70
110
150
190
230
270
20000
16000
12000
8000
4000
0

case 7 TRG(A)

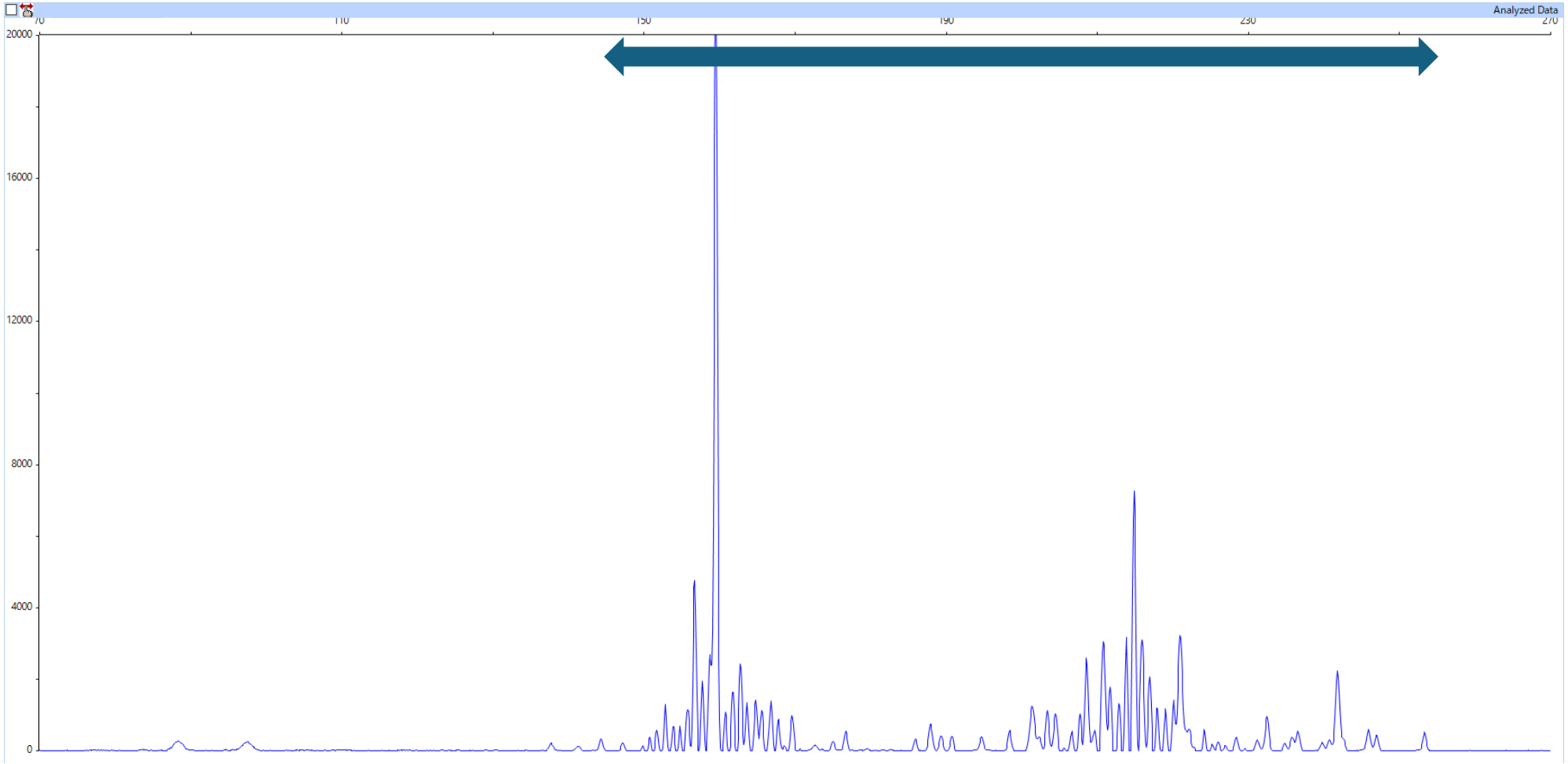
Analyzed Data
70
110
150
190
230
270
20000
16000
12000
8000
4000
0

case 7 TRG(B)

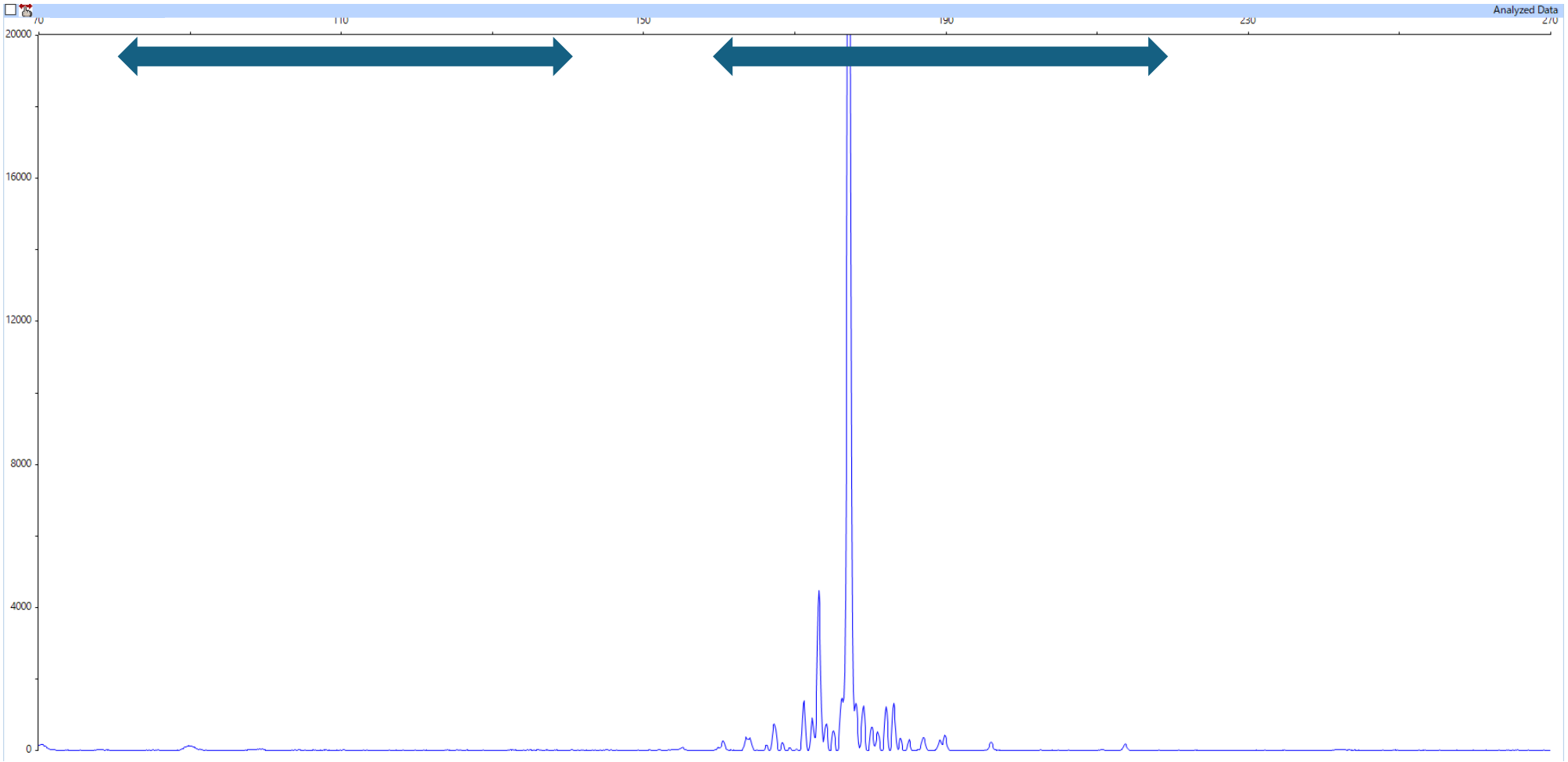
Analyzed Data
70
110
150
190
230
270
20000
16000
12000
8000
4000
0

case 8 TRG(A)

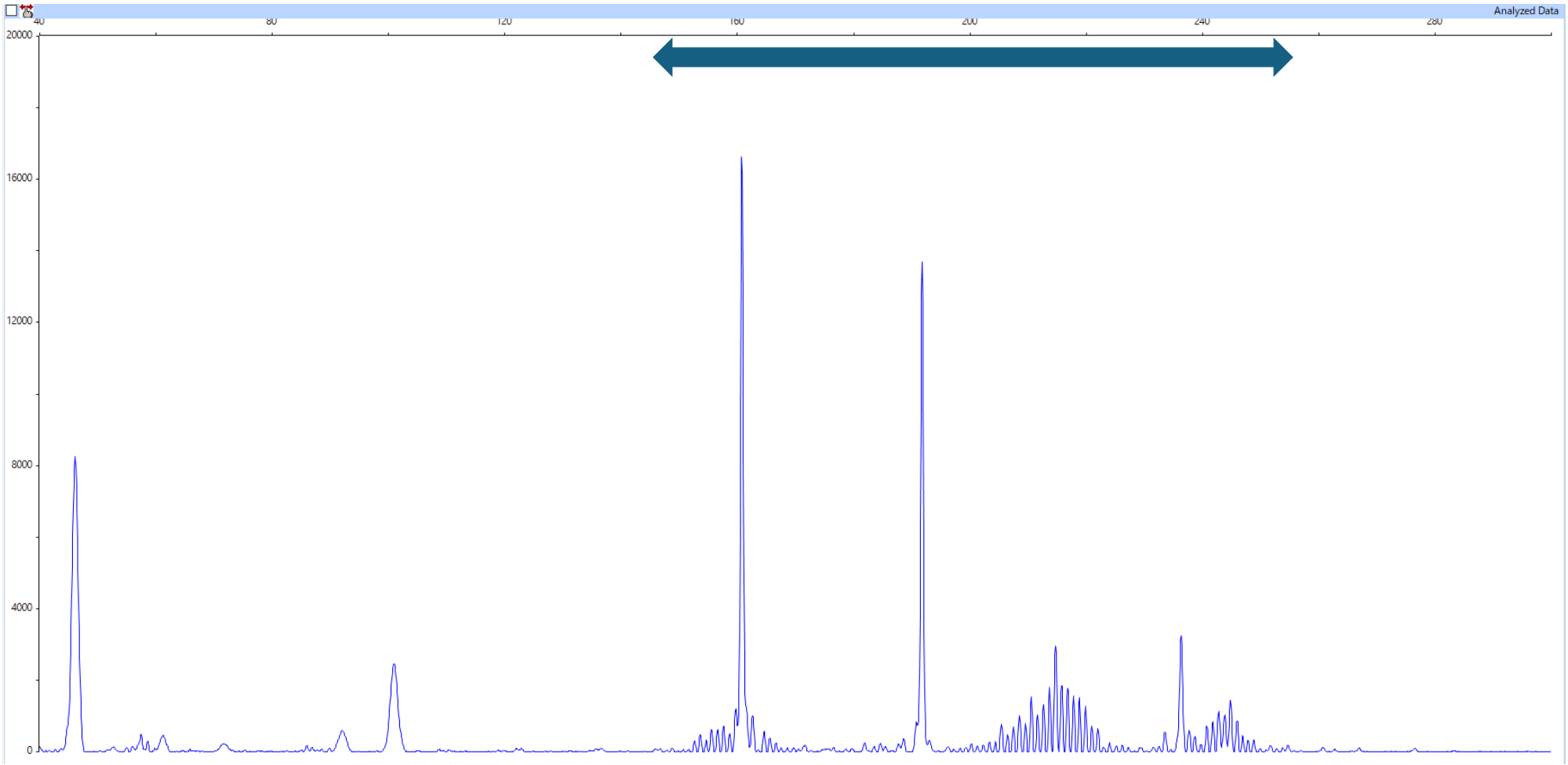
Analyzed Data
40
80
120
160
200
240
280
20000
16000
12000
8000
4000
0

case 8 TRG(B)

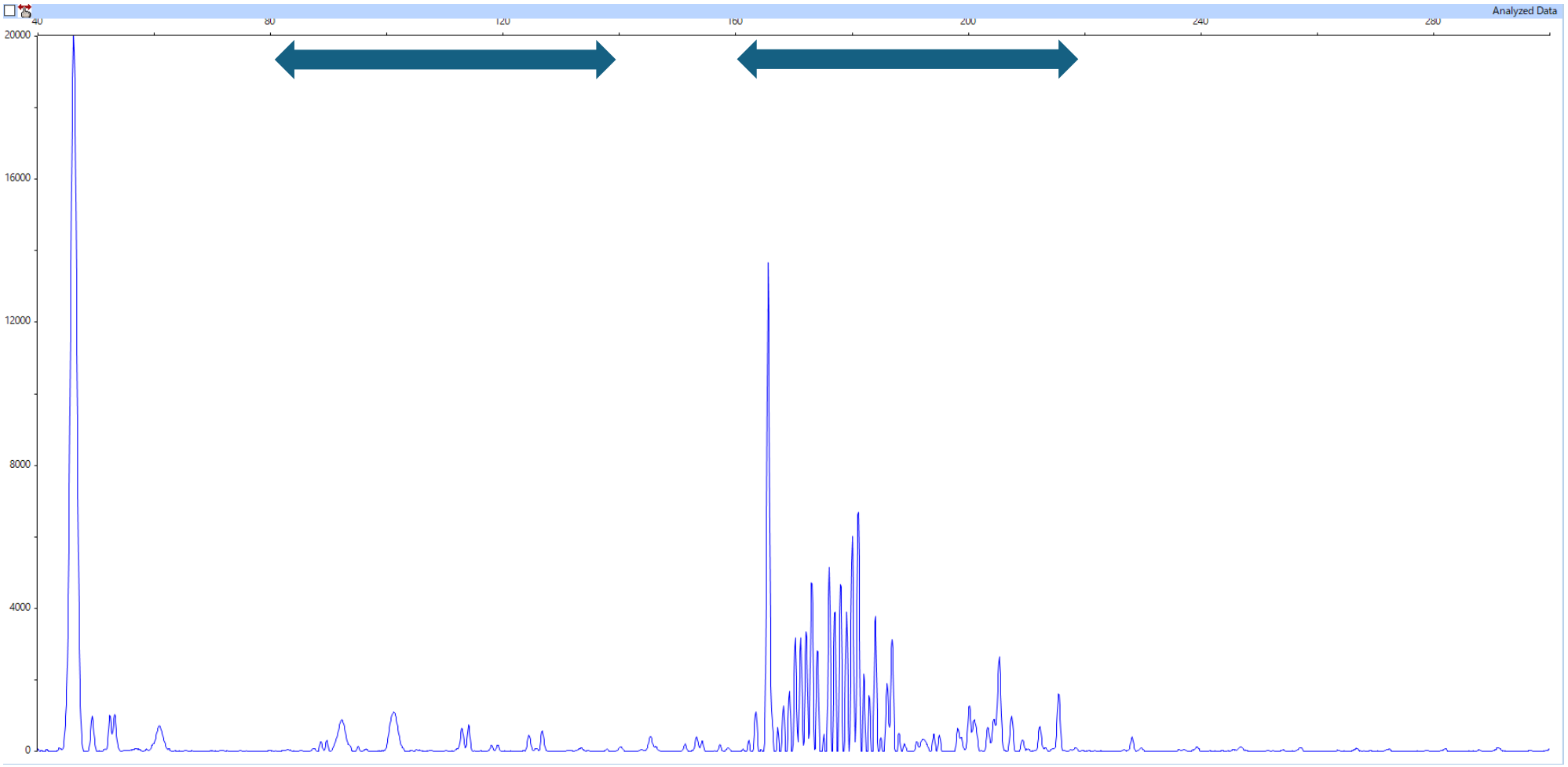
Analyzed Data
40
80
120
160
200
240
280
20000
16000
12000
8000
4000
0

case 9 TRG(A)

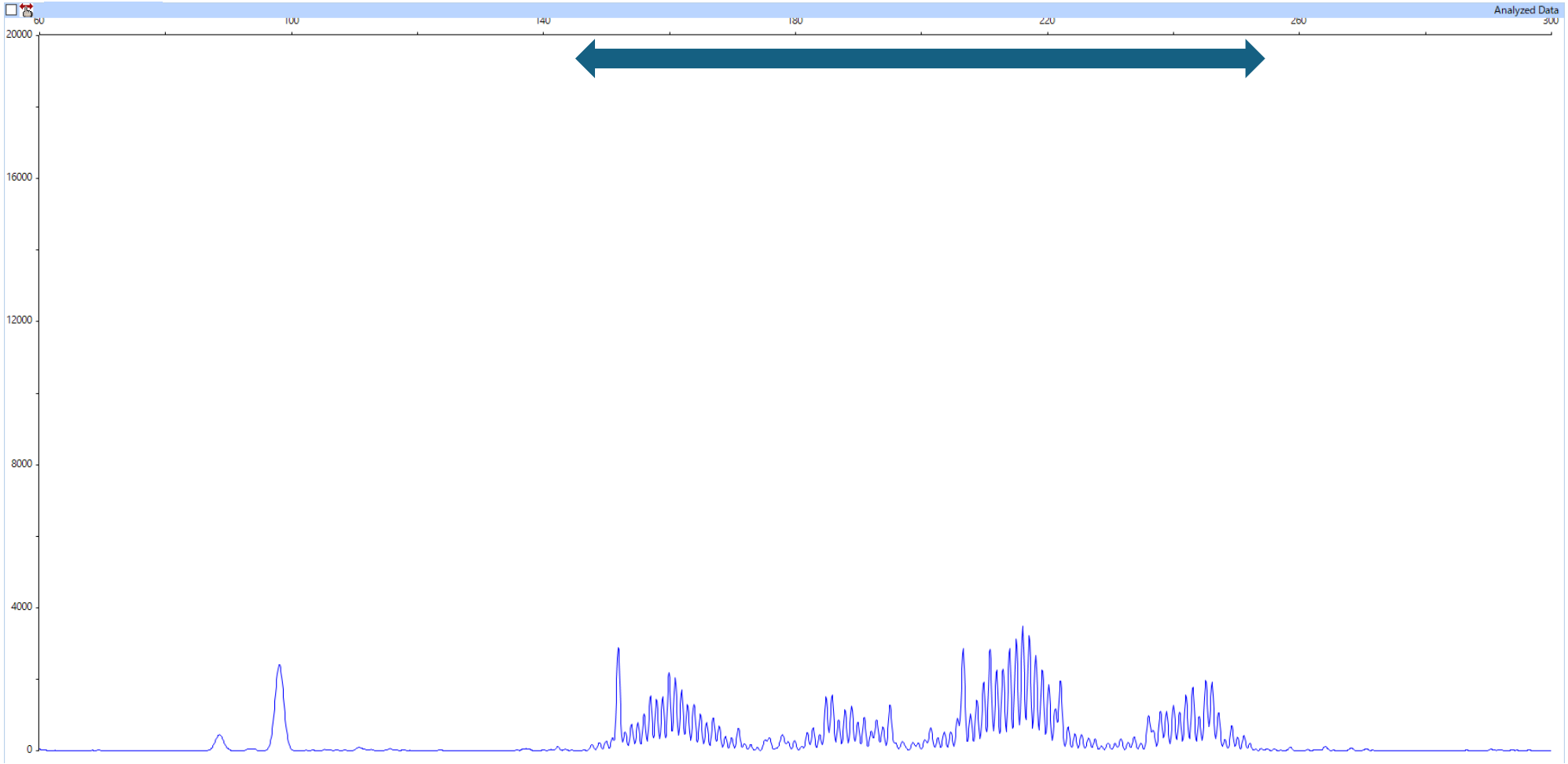
Analyzed Data
60
100
140
180
220
260
300
20000
16000
12000
8000
4000
0

case 9 TRG(B)

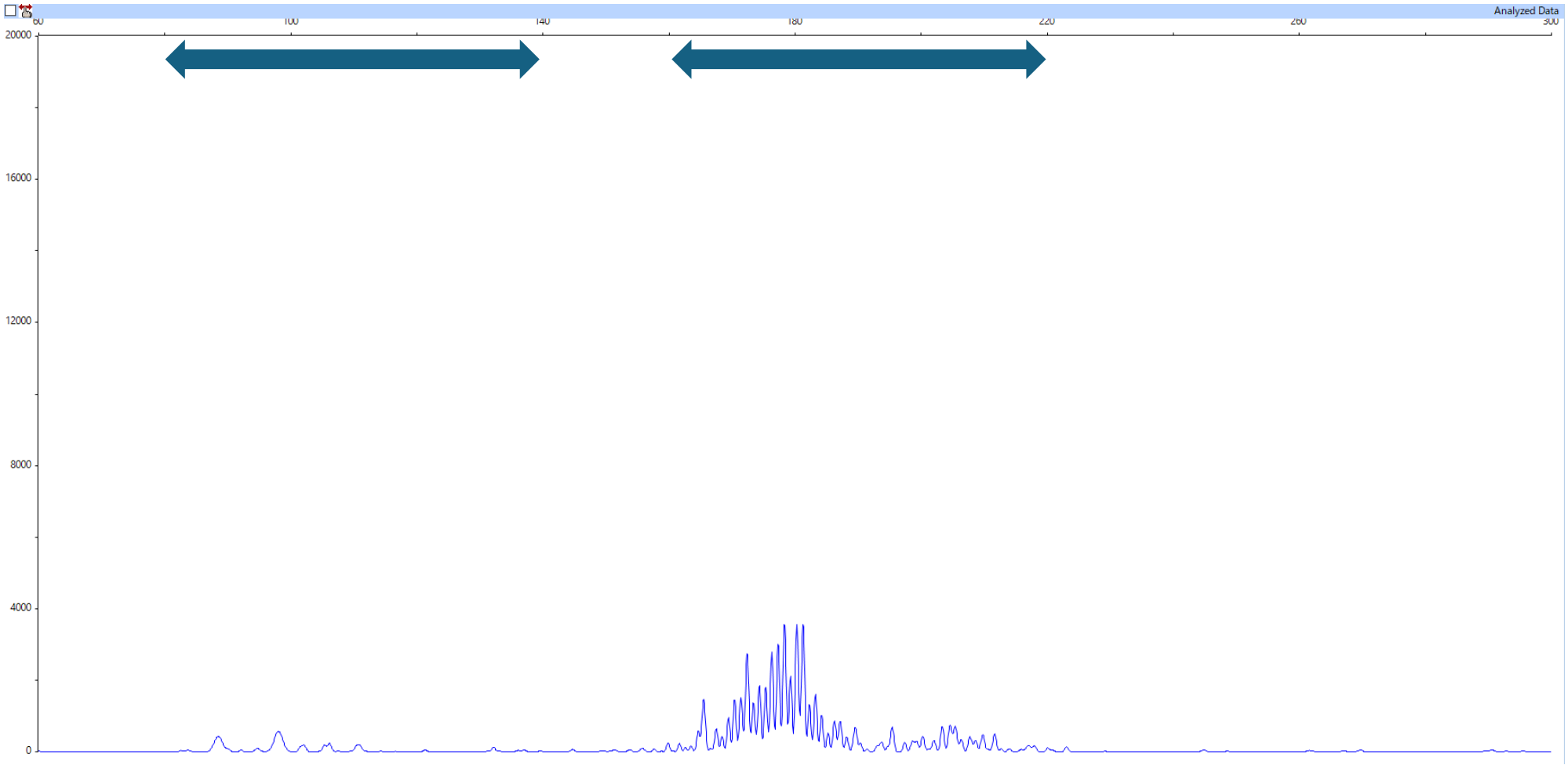
Analyzed Data
60
100
140
180
220
260
300
20000
16000
12000
8000
4000
0

case 10 TRG(A)

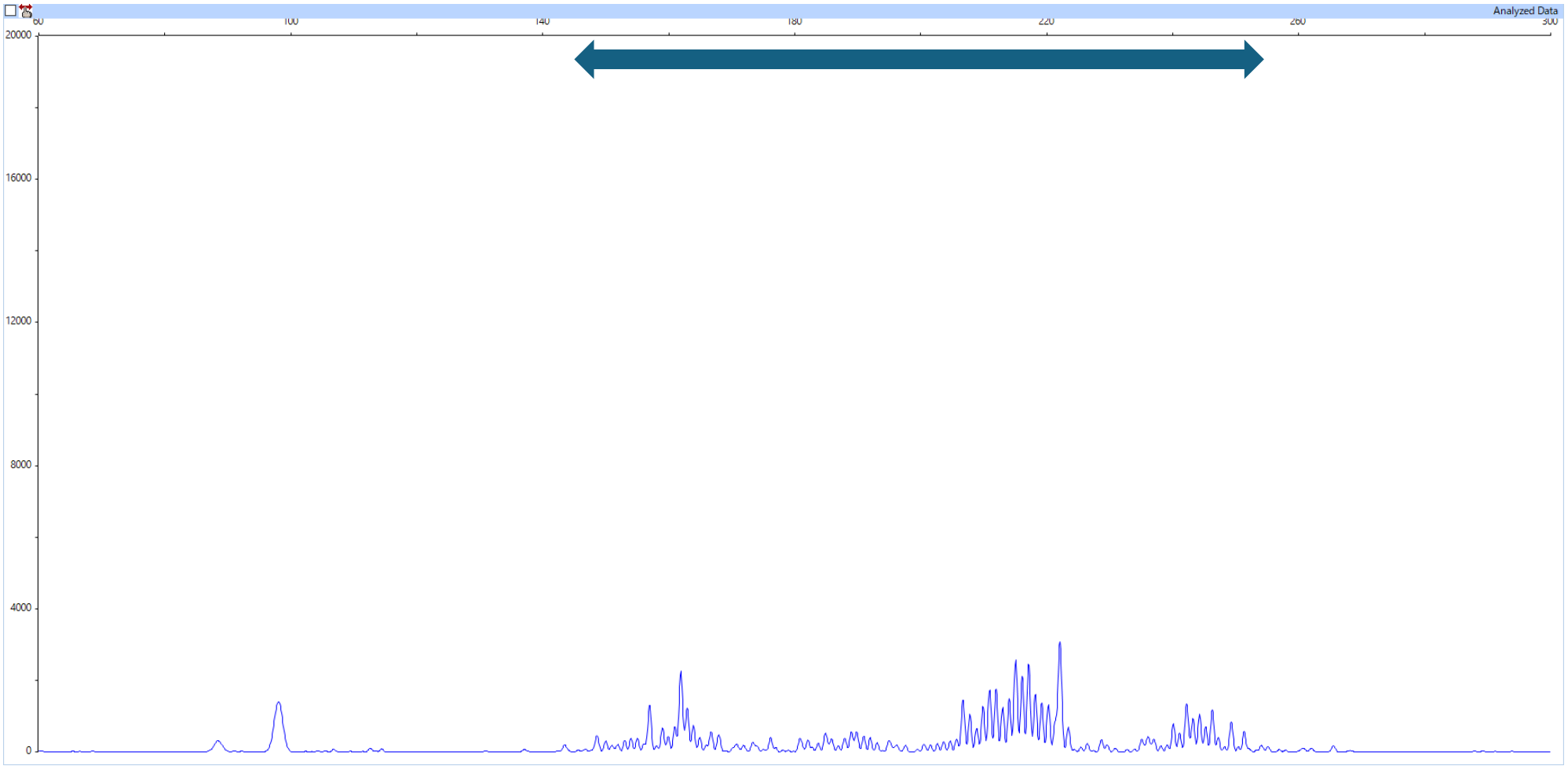
Analyzed Data
60
100
140
180
220
260
300
20000
16000
12000
8000
4000
0

case 10 TRG(B)

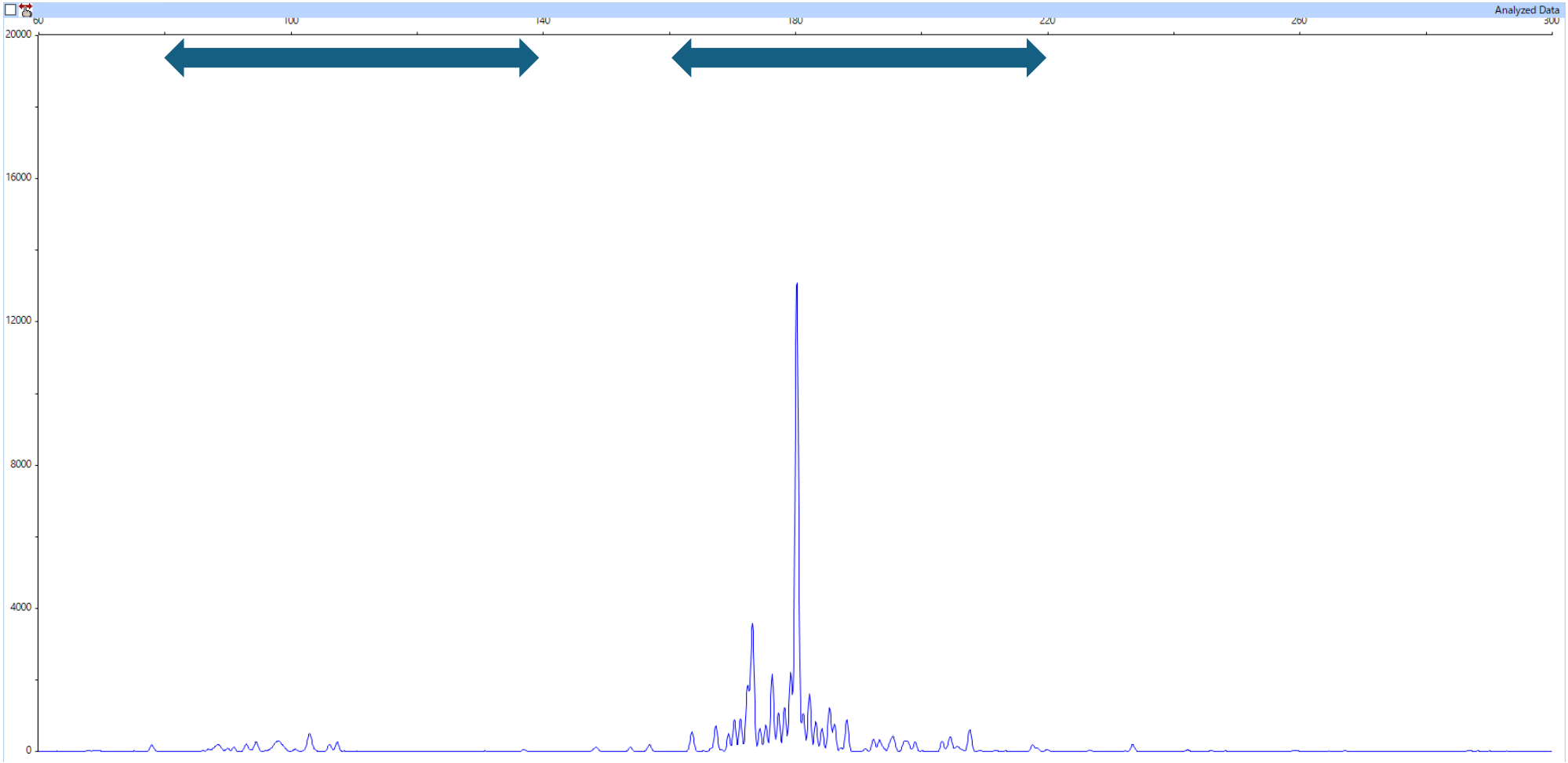
Analyzed Data
60
100
140
180
220
260
300
20000
16000
12000
8000
4000
0

case 11 TRG(A)

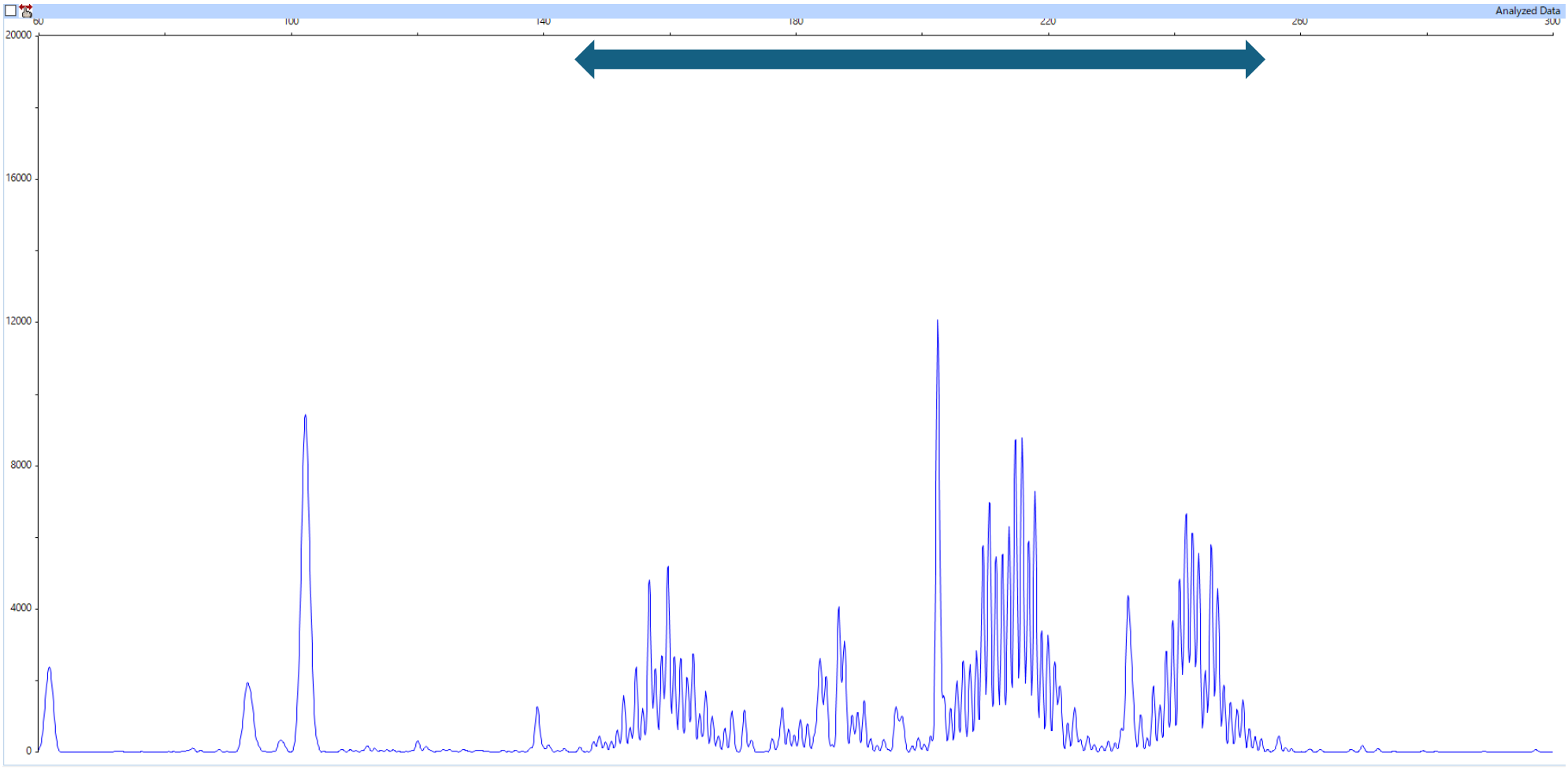
Analyzed Data
60
100
140
180
220
260
300
20000
16000
12000
8000
4000
0

case 11 TRG(B)

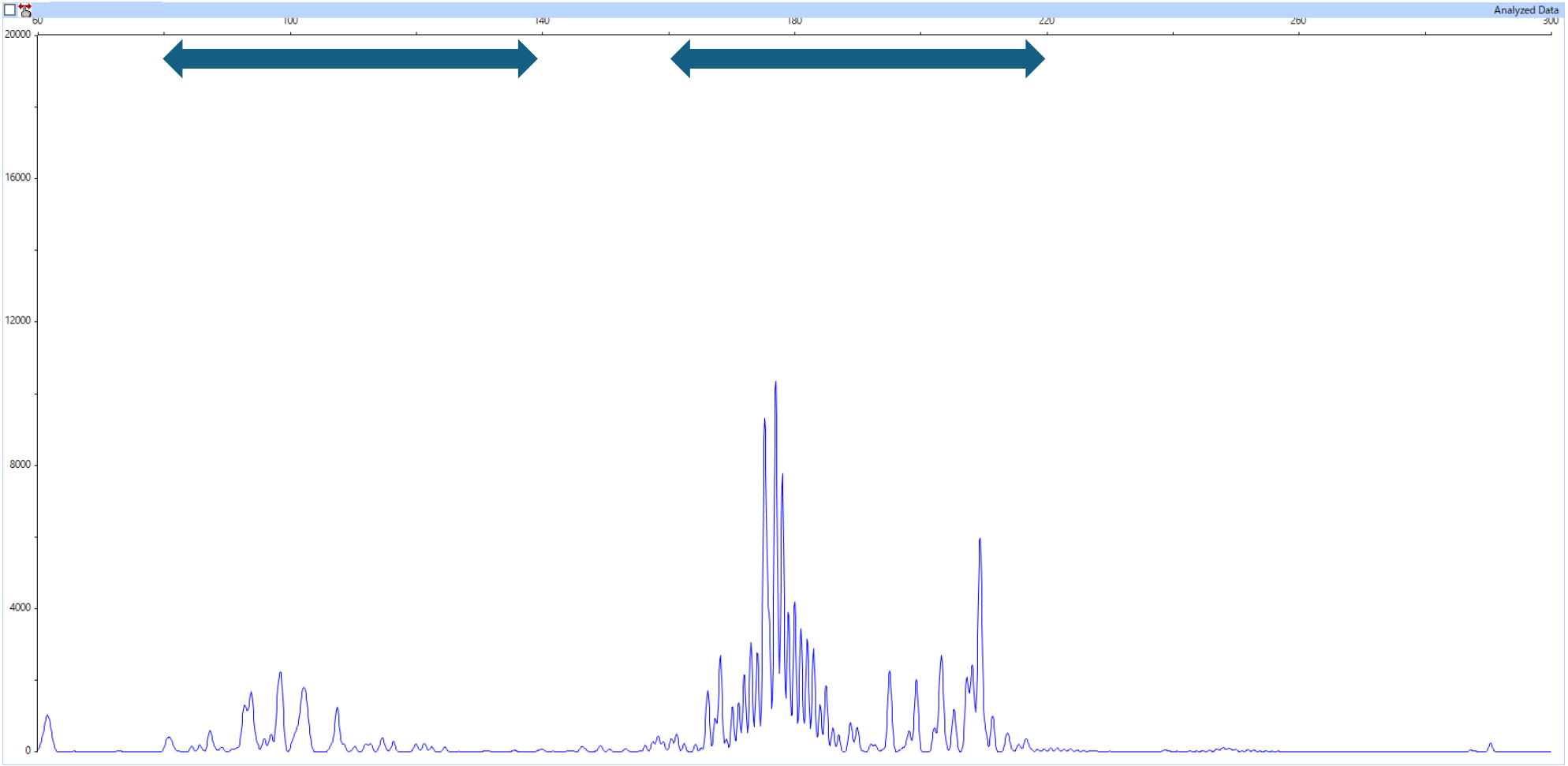
Analyzed Data
60
100
140
180
220
260
300
20000
16000
12000
8000
4000
0

case 12 TRG(A)

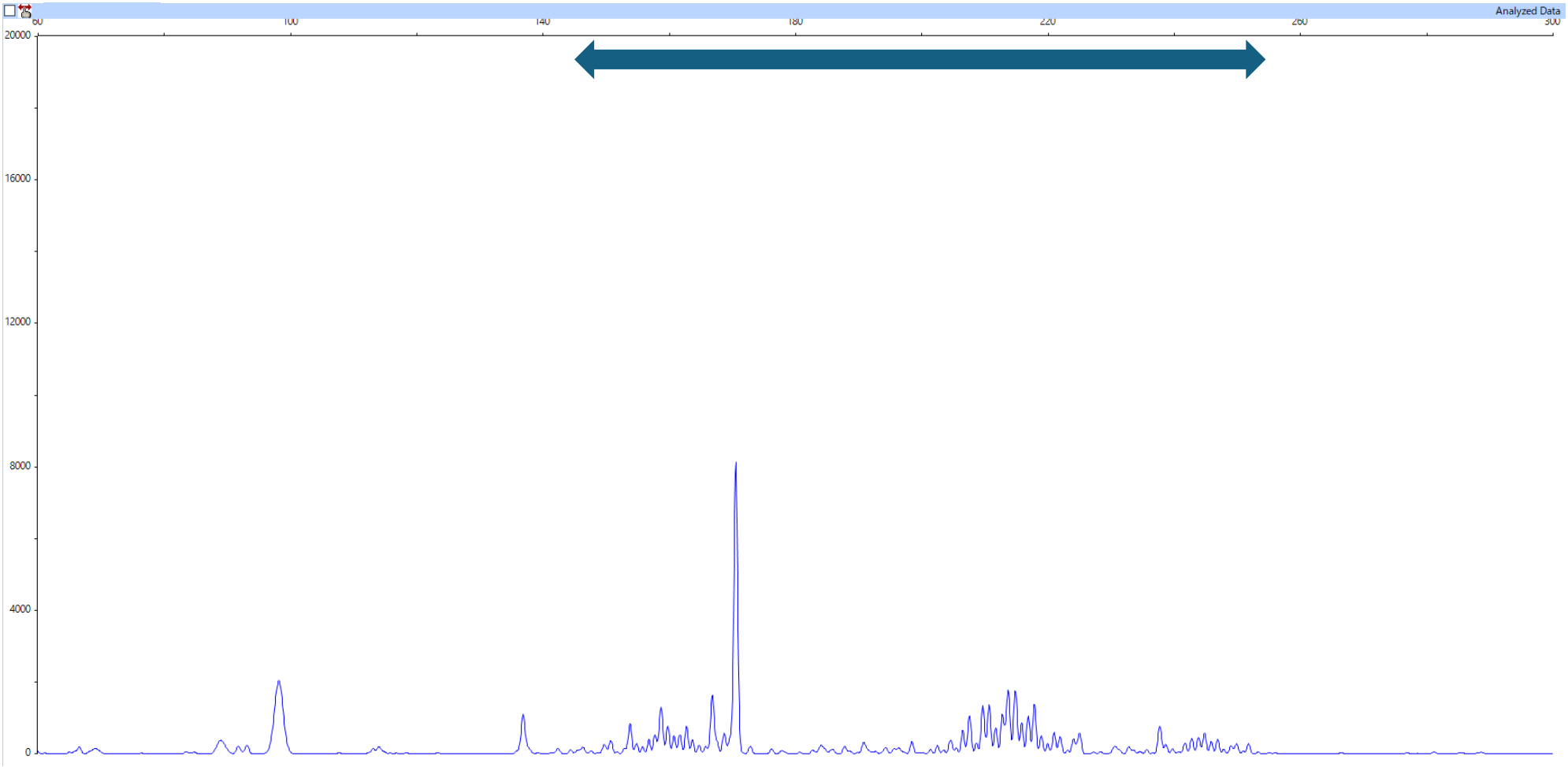
Analyzed Data
60
100
140
180
220
260
300
20000
16000
12000
8000
4000
0

case 12 TRG(B)

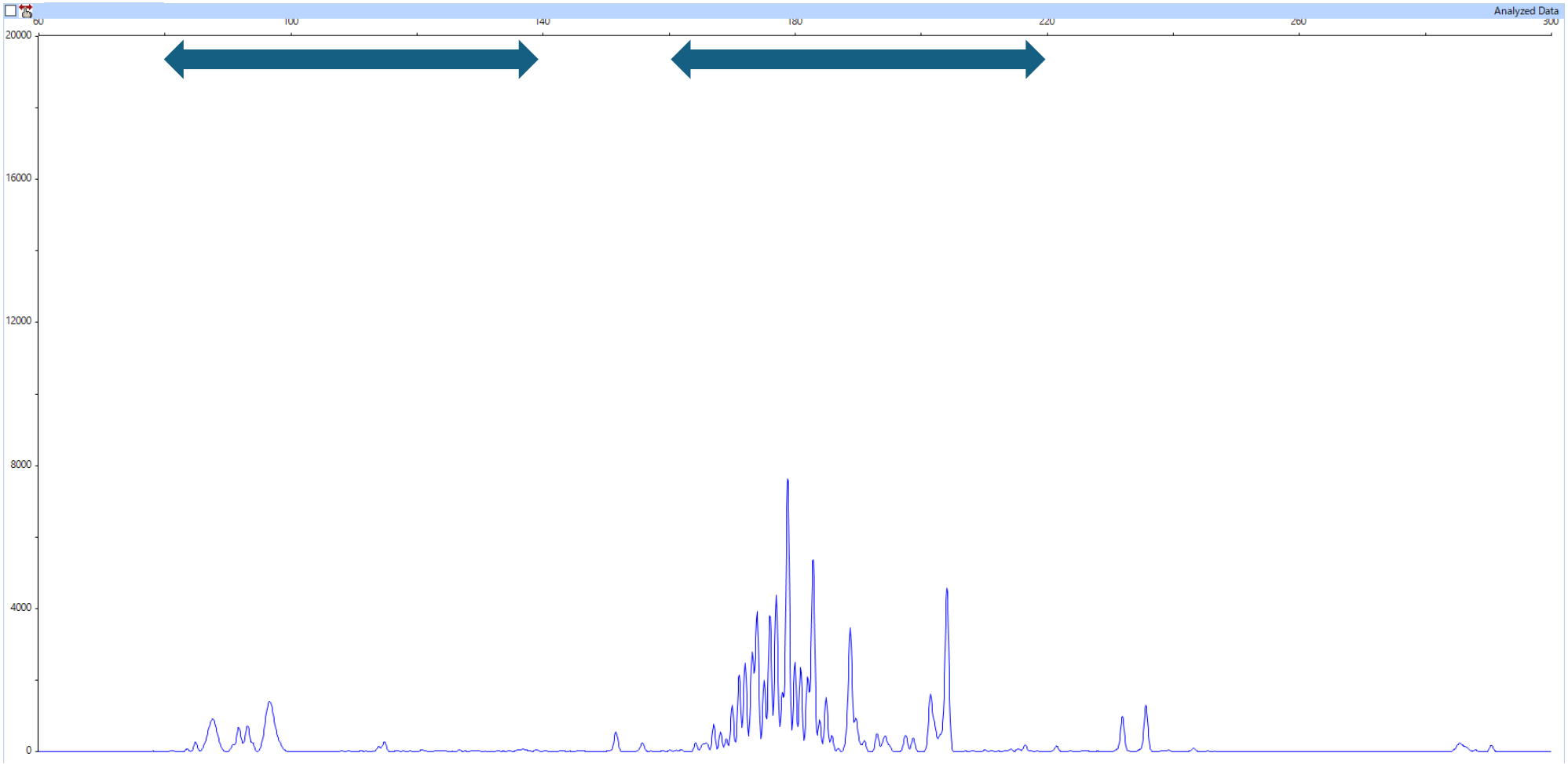
Analyzed Data
60
100
140
180
220
260
300
20000
16000
12000
8000
4000
0